

# SUSTAINABILITY IN ROTATIONAL MOLDING: INFLUENCE OF ADDITIVES

# SUSTAINABILITY IN ROTATIONAL MOLDING: INFLUENCE OF ADDITIVES

By

NIKOL BUDISA, B. Eng.

A Thesis

Submitted to the School of Graduate Studies

In Partial Fulfillment of the Requirements

for the Degree

Master of Applied Science

McMaster University

© Copyright by Nikol Budisa, September 2024

MASTER OF APPLIED SCIENCE  
(Chemical Engineering)

MCMASTER UNIVERSITY  
Hamilton, Ontario

**TITLE:** Sustainability in Rotational Molding: Influence of Additives

**AUTHOR:** Nikol Budisa  
B. Eng. (McMaster University)

**SUPERVISORS:** Dr. Michael Thomspon  
(Chemical Engineering)

**NUMBER OF PAGES:** CXIII, 113

## Abstract

Rotational molding is a polymer processing technique uniquely able to produce large hollow parts while maintaining structural integrity. This benefit comes with a significant drawback: large amounts of plastic waste when a part is defective. The present study aims to investigate the feasibility of recycling rotomolded waste generated in manufacturing facilities in an effort to avoid landfilling and increase sustainability. Long heating times in the presence of oxygen is inherent to the rotomolding process which gives rise to the high likelihood of thermo-oxidative degradation and subsequent deterioration in physical and mechanical properties. These effects are exacerbated during recycling when the polymer is processed multiple times.

To evaluate the impact of degradation two distinct recycling procedures combined various percentages of recycled material (10-50 wt%) with pre-stabilized virgin resin prior to rotomolding. The first recycling procedure exposed polyethylene to a research standard for recycling evaluation whereby multi-pass extrusion is used to promote significant levels of degradation so that the result of degradation may be clearly seen in a recycled polymer. The second technique was a more novel approach to recycling research, where polyethylene resin was repeatedly rotomolded to more closely replicate industrial experiences. In both recycling procedures, the rheological, physical and mechanical properties of recycled samples were found to be similar to the virgin polymer, which may be attributed to the successful protection against thermo-oxidative degradation mechanisms by the additives in the pre-stabilized virgin resin. The most significant change in properties involved the yellowing of the polyethylene samples, most notably when containing 50% recycled content. The discolouration was likely attributed to by-products formed from phenolic antioxidants during the course of protecting the polymer rather than from degradation products themselves since

no mechanical or rheological changes were measured. No reasons were found in this study, due to degradation of properties, for rotomolders to not consider using recycled content when it is present in their facilities; with the caveat that the recycled content must be ground to the same size as the virgin feedstock to maintain comparable sintering performance.

At the end of this thesis, a study was introduced on the stabilizers used in rotomolding grades, with respect to their performance in recycling. A standard antioxidant, UV stabilizer and a pre-stabilized rotomolding-grade resin (as an additive) were each blended with a reactor-grade unstabilized polyethylene resin prior to recycling (by the second technique mentioned above) to investigate their individual and combined effects in reducing degradation. The individual contributions of the antioxidant and UV stabilizer did not show significant variations in polymer properties, although their combined action offered minor yet meaningful improvements in sinterability as well as impact strength, which may indicate a potential synergy and an unintentional benefit that the UV stabilizer provides in alleviating thermo-oxidative degradation effects during rotomolding. A higher concentration of additives may be required in future studies to verify these findings.

## **Acknowledgements**

I would like to express my deepest gratitude to my supervisor, Dr. Thompson, whose support and invaluable guidance have been crucial to the success of this research. Your dedication and expertise have motivated me throughout this journey, and I am sincerely grateful for the opportunity to work under your supervision. I would also like to thank Dr. Vlachopoulos for taking the time to provide me with important insights and feedback that have greatly contributed to my research. Thank you to Imperial Oil Ltd. for providing me with generous financial support, materials and insightful technical guidance. Finally, I would like to extend my thanks to my family, friends and all those who have contributed to my research in any way, whether through discussions, feedback, or moral support. Your contributions have been crucial in the completion of this thesis.

# Table of Contents

Abstract .....	iii
Acknowledgements .....	v
List of Figures .....	xii
List of Tables .....	xvi
1. Chapter 1 Introduction .....	1
1.1. Introduction to Rotational Molding .....	1
1.2. The Need for Recycling in the Rotomolding Industry .....	3
1.3. Research Objectives .....	4
1.4. Thesis Outline .....	4
2. Chapter 2: Literature Review .....	6
2.1. Sources of Recycled Resin in the Rotomolding Industry .....	6
2.2. Degradation in Rotomolding .....	7
2.3. Thermo-oxidative Degradation Reactions .....	10
2.3.1. Chain Scission Reactions .....	13
2.3.2. Crosslinking Reactions .....	14
2.4. Role of additives .....	15

2.4.1.	Primary Antioxidants .....	16
2.4.2.	Secondary Antioxidants .....	17
2.4.3.	UV Stabilizers .....	18
3.	Chapter 3: Rotomolding Process .....	20
3.1.	Apparatus and Procedure .....	20
3.2.	Selection of Operating Conditions in Rotomolding.....	20
4.	Chapter 4: Multi-Pass Extrusion Recycling with HDPE.....	22
4.1.	Introduction.....	22
4.2.	Materials .....	22
4.3.	Methods.....	23
4.3.1.	Recycling Process .....	23
4.3.2.	Melt Flow Index (ASTM D-1238).....	24
4.3.3.	Polymer Sintering Analysis .....	25
4.3.4.	Izod Impact Test (notched) ASTM D256, ISO 180.....	27
4.4.	Results and Discussion .....	28
4.4.1.	Melt Flow Index Results.....	28
4.4.2.	Results of Polymer Sintering .....	29
4.4.3.	Impact Test Results.....	34



4.5.	Conclusions.....	36
5.	Chapter 5: Multi-Step Granulation Recycling with LLDPE .....	37
5.1.	Introduction.....	37
5.2.	Materials .....	37
5.3.	Methods.....	38
5.3.1.	Recycling Process .....	38
5.3.2.	Determining Rotomolding Operating Conditions.....	39
5.3.3.	Dart Impact Test (ASTM D5628).....	41
5.3.4.	Izod Impact (Unnotched) Test ASTM D4812, ISO 180.....	43
5.3.5.	Polymer Sintering Analysis .....	44
5.3.6.	Yellowness Index (ASTM D-1925).....	44
5.3.7.	Rheological Analysis .....	45
5.4.	Results and Discussion .....	46
5.4.1.	Results of Polymer Sintering .....	46
5.4.2.	Results of Impact Tests .....	49
5.4.3.	Rheology Results .....	51
5.4.4.	Yellowness Index Results .....	53
5.5.	Conclusions.....	54
6.	Chapter 6: Recycling Unstabilized HDPE Resin .....	56

6.1.	Introduction.....	56
6.2.	Materials .....	56
6.3.	Methods.....	56
6.3.1.	Sieving Procedure .....	56
6.3.2.	Recycling Process .....	57
6.3.3.	Surface Void Analysis .....	58
6.3.4.	Izod Impact (Unnotched) Test ASTM D4812, ISO 180.....	58
6.3.5.	Yellowness Index Analysis (ASTM D-1925).....	58
6.3.6.	Rheological Analysis .....	58
6.4.	Results and Discussion .....	58
6.4.1.	Rheological Results .....	58
6.4.2.	Results of Surface Void Analysis .....	61
6.4.3.	Izod Impact Strength Results .....	62
6.4.4.	Yellowness Index Results .....	63
6.5.	Conclusions.....	64
7.	Chapter 7: Recycling with HDPE Blends.....	65
7.1.	Introduction.....	65
7.2.	Materials .....	65
7.3.	Methods.....	65

7.3.1.	Recycling Procedure .....	65
7.3.2.	Surface Void Analysis .....	66
7.3.3.	Izod Impact (Unnotched) Test ASTM D4812, ISO 180.....	66
7.3.4.	Yellowness Index (ASTM D-1925).....	66
7.3.5.	Rheological Analysis .....	66
7.4.	Results and Discussion .....	66
7.4.1.	Rheological Results .....	66
7.4.2.	Surface Void Analysis Results.....	68
7.4.3.	Izod Impact Strength Results .....	69
7.4.4.	Yellowness Index Results .....	72
7.5.	Conclusions .....	73
8.	Chapter 8: Additives in Recycling.....	74
8.1.	Introduction.....	74
8.2.	Materials .....	74
8.3.	Methods.....	74
8.3.1.	Additive Compounding Method .....	74
8.3.2.	Recycling Procedure .....	75
8.3.3.	Rheological Analysis .....	79
8.3.4.	Surface Void Analysis .....	79

8.3.5.	Izod Impact (Unnotched) Test ASTM D4812, ISO 180.....	79
8.3.6.	Yellowness Index (ASTM D-1925).....	79
8.4.	Results and Discussion .....	79
8.4.1.	Rheological Results .....	79
8.4.2.	Surface Void Analysis Results.....	81
8.4.3.	Izod Impact Results.....	82
8.4.4.	Yellowness Index Results .....	83
8.5.	Conclusions.....	85
9.	Chapter 9: Final Conclusions and Future Work .....	86
9.1.	Final Conclusions.....	86
9.2.	Future Work .....	88
	References.....	91
	Appendix.....	96

## List of Figures

Figure 1.1. The steps of a typical rotational molding cycle (Crawford and Throne 2002) .....	2
Figure 4.1. A cropped image of the surface of a rotomolded sample containing (A) 0.5% void area and (B) 5.2% void area .....	27
Figure 4.2. MFI for Pass 1-4 extruded HD 8660.29 material with and without the addition of a supplementary antioxidant compared with unprocessed (Pass 0) HD 8660.29 powder.....	29
Figure 2.3. Number of bubbles in the polymer melt plotted with temperature for Pass 2 and Pass 4 HD 8660.29 powders with 30% recycled content compared with unprocessed virgin HD 8660.29 (Pass 0).....	30
Figure 4.4. Number of bubbles in the polymer melt plotted with temperature for Pass 2A and Pass 4A HD 8660.29 powders with 30% recycled content compared with unprocessed virgin HD 8660.29 (Pass 0).....	30
Figure 4.5. Percentage of void area on the surface of the rotationally molded boxes from Passes 1-4 HD 8660.29 with 10, 20 and 30% recycled content compared with virgin HD 8660.29 (Pass 0)	32
Figure 4.6. Percentage of void area on the surface of HD 8660.29 rotomolded samples without antioxidant (Pass 2) and with the addition of antioxidant (Pass 2A) for 10, 20 and 30% recycled content.....	33
Figure 4.7. Percentage of void area on the surface of HD 8660.29 rotomolded samples without antioxidant (Pass 4) and with the addition of antioxidant (Pass 4A) for 10, 20 and 30% recycled content.....	33
Figure 4.8. Izod impact strength for notched rotomolded samples processed using Pass 1-4 HD 8660.29 extruded material with 10, 20 and 30 wt% recycled content.....	34
Figure 4.9. Impact strength of Pass 2 HD 8660.29 rotomolded material with and without the addition of Irganox 1010 antioxidant.....	35
Figure 4.10. Impact strength of Pass 4 HD 8660.29 rotomolded material with and without the addition of Irganox 1010 antioxidant.....	35

Figure 5.1. Surface void area of LL 8555.25 rotomolded samples with various PIATs and oven temperatures.....	40
Figure 5.2. MFE of LL 8555.25 rotomolded samples with various PIATs and oven temperatures 41	
Figure 5.3. Number of bubbles in the polymer melt plotted with temperature for Regrind 1-4 LL 8555.25 powdered material with 30% recycled content compared with virgin LL 8555.25 (Regrind 0) 47	
Figure 5.4. Number of bubbles in the polymer melt plotted with temperature for Regrind 3 LL 8555.25 powder containing 30 and 50% recycled content .....	48
Figure 5.5. Percentage of void area on the surface of the LL 8555.25 rotationally molded boxes from Regrind 1-4 with 10, 30 and 50% recycled content compared with virgin LL 8555.25 (Pass 0) 49	
Figure 5.6. Izod impact strength for unnotched specimens taken from Regrind 1-4 LL 8555.25 rotomolded samples with 10, 30 and 50% recycled content.....	50
Figure 5.7. Complex viscosity for LL 8555.25 Regrind 4 samples with 10, 30 and 50% recycled content compared to a rotomolded sample with virgin LL 8555.25 .....	52
Figure 5.8. Cole-Cole plot for LL 8555.25 Regrind 4 rotomolded samples with 10, 30 and 50% recycled content, compared with a virgin LL 8555.25 rotomolded sample .....	52
Figure 5.9. Yellowness Index for LL 8555.25 Regrind 1-4 rotomolded samples with 10, 30 and 50% recycled content compared with a virgin LL 8555.25 (Regrind 0) sample.....	54
Figure 6.1. Particle size distribution of RG8660 resin compared with HD 8660.29 resin .....	57
Figure 6.2. Complex viscosity with increasing angular frequency for RG8660 Regrind 1-3 samples compared with virgin RG8660.....	59
Figure 6.3. Cole-Cole plot for RG8660 Regrind 1-3 samples compared with a virgin RG8660 sample (Regrind 0).....	60

Figure 6.4. Surface void area of RG8660 Regrind 1-3 rotomolded samples compared with virgin RG8660 (R0).....	61
Figure 6.5. Izod impact strength for RG8660 Regrind 1-3 rotomolded samples with 30% recycled content compared to virgin RG8660 (R0) .....	62
Figure 6.6. Yellowness Index for RG8660 Regrind 1-3 rotomolded samples compared with a rotomolded virgin RG8660 sample (R0) .....	64
Figure 7.1. Complex viscosity of a rotomolded RG8660 R2 sample compared to an HD Blend R2 sample .....	67
Figure 7.2. Cole-Cole plot for a rotomolded RG8660 R2 sample compared with an HD Blend R2 sample .....	68
Figure 7.3. Surface void analysis for Regrind 0-2 samples made with HD Blend compared with RG8660 .....	69
Figure 7.4. Izod impact strength for Regrind 0-2 samples processed using a 30/70 blend of HD 8660 resin and unstabilized RG8660 resin, and compared with samples processed with unstabilized resin (RG8660).....	71
Figure 7.5. YI for all HD Blends compared with RG8660 samples .....	72
Figure 8.1. Microscopic images with a 6x magnification level of (A): powder obtained via the grinding mill with a 0.5 mm sieve of extruded sample “ANT” and (B): RG8660 powdered resin obtained from supplier .....	78
Figure 8.2. Photo of a rotomolded box processed using: (A) 100% powder obtained via the grinding mill with a 0.5 mm sieve of extruded sample “ANT” and (B) a blend of 70 wt% virgin RG8660 powder and 30 wt% of ground “ANT” powder obtained from the grinding mill .....	78
Figure 8.3. Complex viscosities for all stabilized rotomolded samples subject to Regrind 2 (R2) compared with a RG8660 R2 sample .....	80
Figure 8.4. Cole-Cole plot for all stabilized rotomolded samples subject to Regrind 2 (R2) compared with a RG8660 R2 sample .....	81

Figure 8.5. Surface void analysis for all stabilized rotomolded samples compared with RG8660 samples.....	82
Figure 8.6. Izod impact strength for all of stabilized rotomolded samples compared with RG8660 samples.....	83
Figure 8.7. YI for all rotomolded stabilized samples compared with RG8660 samples .....	84
Figure 1A. Screw design used for melt compounding additives with RG8660 polymer, as discussed in Section 8.3.1. ....	96



## List of Tables

Table 4.1. Naming convention of rotomolded samples from multi-pass extrusion recycling with HD 8660.29.....	24
Table 5.1. Rotomolded sample naming convention in multi-step granulation recycling with LL 8555.25.....	39
Table 5.2. MFE for Re grind 4 samples containing 10, 30 and 50% recycled content compared with a virgin LL 8555.25 sample (Re grind 0), along with the number of brittle failures observed .....	51
Table 6.1. Rotomolded sample naming convention in multi-step granulation recycling with RG8660 .....	58
Table 6.2. Percentage of ductile and brittle fractures observed during unnotched Izod testing for RG8660 rotomolded samples.....	63
Table 7.1. Summary of the naming convention for HD Blend rotomolded samples.....	66
Table 7.2. Percentage of ductile fractures observed during unnotched Izod testing for all HD Blend samples compared with RG8660 rotomolded samples .....	71
Table 7.3. Percentage of brittle fractures observed during unnotched Izod testing for all HD Blend samples compared with RG8660 rotomolded samples .....	71
Table 8.1. Components of formulations 1-3 along with their respective weight percentages and extruded formulation sample names .....	75
Table 8.2. Summary of stabilized rotomolded sample naming convention.....	76

# Chapter 1 Introduction

## 1.1. Introduction to Rotational Molding

Rotational molding, also known as rotomolding, is a polymer processing technique used to manufacture a variety of hollow plastic products. In recent years, rotomolding has gained popularity and is currently utilized in various industries such as automotive, agriculture, recreation, and construction.

The rotomolding process can be broken down into four basic steps, illustrated in Figure 1. The steps are as follows.: (i) The mold is charged at ambient temperature and pressure with a pre-defined weight of fine polymer powder, typically measuring less than 500 microns in particle size. The charged mold is then securely closed and clamped into place while slowly rotating along two axes perpendicular to one another. (ii) The charged mold is placed in an oven allowing for the polymer to slowly heat up while in rotation. During this stage, the polymer powder begins to melt and adhere to the walls of the mold. A homogenous layer of molten polymer forms along the entire inner surface of the mold. (iii) Once melting is completed and the polymer has uniformly coated the mold, the mold is removed from heat. The mold is then cooled slowly with the help of blown air or sprayed water while still in rotation to retain the shape of the mold. (iv) When cooling is completed, the final part is carefully removed from the mold (Crawford and Throne 2002).

Compared to alternative polymer molding techniques such as blow molding, thermoforming and injection molding, rotational molding has few competitors capable of producing large hollow parts greater than 2 m<sup>3</sup> as a single piece while maintaining exceptional uniformity. Additional unique advantages specific to rotational molding include its use of relatively inexpensive molds and the ability to produce seamless, stress-free products without the presence of weld lines. Despite these advantages, the nature of the rotational molding process presents significant limitations such

as large amounts of scrap when a part is off-spec, and slower heating and cooling rates compared to blow molding and injection molding, resulting in considerably longer cycle times (Crawford and Throne 2002). Prolonged polymer exposure to high temperature environments gives rise to polymer degradation mechanisms which can alter the polymer structure and lead to detrimental effects in physical and mechanical properties (Cuadri and Martín-Alfonso 2017). These effects are exacerbated when the polymer undergoes the rotomolding cycle multiple times, such as in the case of recycling.

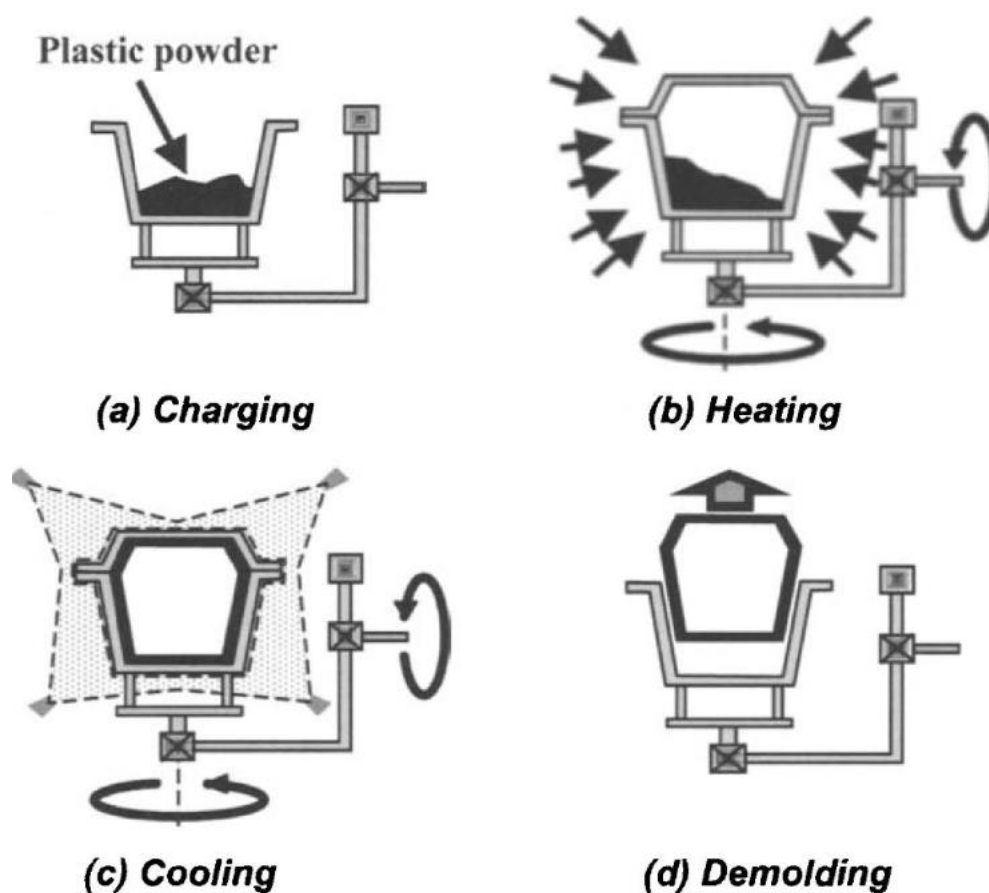


Figure 1.1. The steps of a typical rotational molding cycle (Crawford and Throne 2002)

## 1.2. The Need for Recycling in the Rotomolding Industry

With the global demand for plastics continually on the rise, there is a critical need for sustainable approaches to address environmental challenges associated with plastic waste. The rotational molding industry is actively involved in manufacturing plastic products that can reach sizes as large as 20,000 gallons. Due to the substantial size of these products, the rotomolding industry produces a considerable amount of plastic waste, emphasizing the need for recycling initiatives within its processes.

Plastic recycling not only offers environmental benefits by diverting waste from landfills and promoting energy efficiency, but it also offers economical advantages by reducing raw material costs for manufacturers. Thus, it is important to find ways to implement recycling in rotomolding to attain a more sustainable future.

The main challenge with recycling in the rotomolding industry is the long heating cycle inherent to the process which can diminish product quality. Rotomolded products often require high durability and consistency which can be difficult to achieve through recycling where the polymer is repeatedly exposed to high temperatures for long periods of time, promoting notable polymer degradation. The source of the polymer for recycling defines the scale of this challenge, where **regrind resin** created and remaining within a rotomolding facility has an understood processing history and level of contamination whereas **post-consumer reclaim** (blue bin waste) can be exposed for a long period to multiple degradation initiators (e.g. heat, chemicals, UV light) upon leaving the manufacturing facilities and subject to considerable contamination while being used. The present research is limited to regrind recycling, which will still have a significant impact on waste diversion from landfill sites.

### **1.3. Research Objectives**

The first objective for this project is to examine physical, mechanical and rheological characteristics of polymers subjected to two distinctly different approaches for evaluating the feasibility of recycling polyethylene regrind in order to detect and quantify signs of polymer degradation. The traditional multi-pass approach was first tested where the much higher stress state of an extruder is used to promote significant and differing levels of degradation in the polymer resin before rotomolding, versus a newer approach devised in this project was reliant solely on repeated rotomolding trials that more closely replicates industrial experiences.

The second objective for this project is to investigate the role that different additives play in protecting polymers during the course of recycling in rotational molding. A standard antioxidant and/or UV stabilizer will be incorporated in reactor-grade, unstabilized polyethylene resin to study their individual and combined roles in preventing degradation during recycling. In addition, a polyethylene blend consisting of the unstabilized resin mixed with a commercial rotomolding-grade resin with typical amounts of one or both types of additives will undergo the recycling process in order to assess the effectiveness of each additive in managing degradation effects.

### **1.4. Thesis Outline**

This thesis is divided into 9 chapters including the Introduction. Chapter 2 focuses on a literature review consisting of the type of degradation that may take place during a rotational molding process, the specific reaction mechanisms that arise, and the role that various additives play in mitigating polymer degradation. Chapter 3 outlines the rotomolding apparatus and fundamental procedure used for all rotomolding experiments in this thesis, along with the selection of operating conditions. The remaining chapters, aside from the conclusion, consist of distinct rotomolding recycling studies conducted, including a brief introduction, methodologies used, as

well as experimental results and discussions. Chapter 4 presents results for the multi-pass extrusion recycling study conducted with a highly stabilized commercial resin while Chapter 5 presents results from the alternative recycling approach involving multi-step granulation with a less stabilized polymer resin. Chapters 6-8 consist of a multi-step granulation recycling study involving the reactor-grade unstabilized resin, a polyethylene blend, and the incorporation of various additives into the unstabilized resin, respectively. Lastly, an overall conclusion of regrind recyclability in rotational molding for polyethylene, as well as suggestions for future work, will be presented in Chapter 9.

## **Chapter 2: Literature Review**

### **2.1. Sources of Recycled Resin in the Rotomolding Industry**

Two main waste streams exist in the plastics industry. The first is post-industrial recycled material (PIR), normally known as regrind, which includes waste that is produced during the production process and does not leave the facility, such as surpluses or trimmings. The second waste stream is post-consumer recycled material (PCR), otherwise known as post-consumer reclaim, which presents more complex challenges for recycling. This includes waste derived from households or commercial facilities that have reached their end-use and are no longer suitable for their original purpose.

The complexity of using PCR for recycling in rotomolding is mainly due to a part's composition, the thermal history of the polymer(s) and difficulties with sourcing. It is crucial that resin used in rotomolding possesses very specific characteristics such as high thermal stability and good flowability so that the rotomolding cycle isn't too long and the polymer can withstand the conditions without loss in properties (Crawford and Throne 2002). For this reason, polyethylene is almost exclusively used in rotomolding, with polypropylene used less frequently. These resins are also chemically optimized for rotomolding through the use of stabilizers, implying that not all polyethylene and polypropylene sources are suitable for rotomolding. Presently, PCR is only sorted into two main categories, polyethylene or polypropylene, whichever is the dominant component in the part. Sorting does not consider the thermal histories of the polymers which may have chemically modified them to a point where they are no longer suitable to be rotomolded. Dvorak (2016) studied the applicability of HDPE PCR for rotomolding and found that HDPE originally manufactured by extrusion blow molding cannot be used in rotomolding due to significant rheological changes of the material, although in recent years this idea has increasingly

been challenged by the rotomolding industry. Recent recommendations have been made to implement a new recycling label intended solely for rotomolded PCR in an effort to boost recycling within the rotomolding industry. However, even with the implementation of a new recycling label, the relatively small rotomolding market size, coupled with the longevity of rotomolding products makes it difficult to source true rotomolded PCR (Turgeon 2024).

Due to the complexities associated with PCR in rotomolding and understanding this industry is quite leery of recycled materials, in general, due to the large costs associated with making off-spec parts, the recycling methods studied in this thesis are intended to provide insight on the recyclability of PIR only. With the rotomolding industry producing products of substantial sizes, the amount of recyclable plastic from PIR is significant and will have a dramatic impact on improving sustainability. Currently, it is estimated that approximately 30% of rotational molding companies use some level of PIR into their processes, with the percentage of PIR varying from 10-50%. The exact percentage of PIR depends on both the quality of the recycled resin as well as the desired properties of the final product (Turgeon 2024).

## **2.2.Degradation in Rotomolding**

Polymer degradation involves the chemical modification of a polymer structure typically resulting in undesirable changes in the performance characteristics of the material (Horie et al. 2004). Polymers degrade through various mechanisms depending on molecular parameters along with the processing environment to which the polymer is exposed. The onset of these mechanisms is due to high processing temperatures combined with exposure to oxygen or relevant mechanical stresses.



Thermo-mechanical degradation arises when high temperatures in combination with high shear stresses are applied to the polymer, such as in the case of extrusion and injection molding. Research has shown that thermo-mechanical degradation often results in the scission of polymer chains leading to a reduction in molecular weight and adverse effects on mechanical properties (Odell, Keller, and Muller 1992). This type of degradation is potentially relevant in the case of multi-pass extrusion recycling where the polymer is repeatedly processed through an extruder with the intention to increase its susceptibility to degradation during rotational molding, usually for experimental studies like the present project. However, the presence of oxygen during the extrusion process also gives rise to thermo-oxidative degradation which has been proven to have a more significant impact on polymer properties compared to thermo-mechanical degradation. Billiani et al. (1990) studied the effects of molecular degradation during injection molding and found that significant reduction in molecular weight was mainly caused by thermo-oxidative effects as opposed to high shear stresses. Efforts have been made by Rideal and Padget (1976) to purge polymer processing equipment with an inert gas in an effort to eliminate the oxygen present in the system; however, oxidation reactions were still observed in the final product. Epacher et al. (2000) determined that oxygen adsorbs onto the surface of polymer powder and that an equal or greater amount of oxygen is dissolved into the polymer matrix, ranging from 40-70 ppm. Thus, oxygen remains present during extrusion processes, even when attempts are made to purge the system with an inert gas, allowing for thermo-oxidative degradation to take place and prevail over thermo-mechanical degradation.

In the case of rotomolding, the shear stresses applied to the polymer are minimal, therefore the primary source of polymer degradation is thermo-oxidative degradation. The hollow mold inherent to the rotational molding process results in direct exposure of the polymer melt to an

oxygen-rich environment during heating, which initiates thermo-oxidative degradation. Cramez et al. (2003) studied degradation during the rotational molding process for polyolefins and concluded that polymer degradation occurs primarily at the inner surface of the polymer which is in direct contact with air for the longest period of time. Although the temperature of the inner surface of the polymer is lower than at the mold wall, the direct exposure to oxygen has a significant impact in accelerating the degradation process (Cramez, Oliveira, and Crawford 2003).

Many researchers have found that the extent of degradation experienced by the polymer during rotomolding is heavily correlated with the heating time during the process, typically expressed as the peak internal air temperature (PIAT) that is reached during processing (Ogila et al. 2017). A PIAT that is too high results in an excessive exposure of the polymer amid high temperatures, accelerating thermo-oxidative degradation reactions, while a PIAT that is too low results in an under-cooked part, unable to fully sinter, resulting in mechanical losses (Sharifi et al. 2012). Thus, the PIAT selected for processing should be low enough where degradation effects are not dramatic, but still high enough where the polymer's sintering ability is not compromised (Ogila et al. 2017).

The effect of heating time on polymer structure and impact performance of HDPE during rotomolding was studied by Chen et al. (2019) and it was discovered that an increase in heating time from 21 to 25 minutes resulted in a dramatic decline in impact strength of the rotomolded part as well as signs of brittle behaviour. Additionally, polarizing micrographs captured morphological changes in the inner layer of rotationally molded samples subject to different heating times. It was found that when a heating time of 23 minutes was increased to 28 minutes, the size of the spherulites in the inner surface of the polymer slightly increased, suggesting that degradation effects were more prominent at the polymer's inner surface compared to at the mold

wall (L. Chen et al. 2019). Similar observations were made by Oliveira and Cramez (2001), who concluded that a PIAT above the critical point during rotomolding is directly related to the extent of thermo-oxidative degradation of the polymer. Clear morphological changes at the inner surface of polyethylene, confined to a layer approximately 30  $\mu\text{m}$  deep, were observed as degradation increased. These changes involved a decrease in the size and uniformity of spherulites at the inner surface of the polymer. In addition to morphological changes, the impact strength of the rotomolded samples subjected to PIATs above the critical point significantly decreased and resulted in brittle behaviour (Oliveira and Cramez 2001). Umbare and Arakerimath (2024) also investigated the effect of various PIATs on mechanical properties of linear low density polyethylene (LLDPE) during rotomolding. They found that a PIAT of 200  $^{\circ}\text{C}$  was too high and resulted in polymer degradation where the flexural strength and flexural modulus were severely compromised compared to a PIAT of 190  $^{\circ}\text{C}$ . Similarly, Sharifi et al. (2012) demonstrated that linear medium density polyethylene exhibited a catastrophic loss in mechanical properties due to thermo-oxidative degradation when the heating time of the polymer was raised from 11 minutes to 13 minutes during rotomolding.

### **2.3. Thermo-oxidative Degradation Reactions**

A general thermal oxidation mechanism for rubbers, originally developed by Bolland and Gee (1946), has since been adapted to describe the thermo-oxidative degradation mechanism specific to polyolefins (Gijssman 2008). This mechanism involves a three-step chain process consisting of initiation, propagation and termination steps.

Initiation begins when the energy input from heat results in a homolytic scission reaction of an arbitrary carbon-carbon or carbon-hydrogen bond along the polymer chain, resulting in the

formation of an unstable alkyl radical (Reaction 1). In Reaction 1, RH represents a polymer molecule and R $\cdot$  represents an alkyl radical

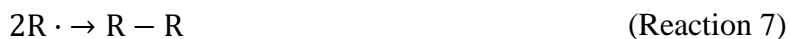


Following initiation, oxygen from the environment surrounding the polymer then reacts with the alkyl radical to form a peroxy radical (RO $_2\cdot$ ) (Reaction 2). The peroxy radical abstracts a hydrogen atom from neighbouring polymer chains, resulting in the formation of a hydroperoxyl molecule (ROOH) and a new free radical (Reaction 3). Due to the instability of hydroperoxyl molecules, decomposition arises to produce additional radicals (Reaction 4) where RO $\cdot$  and OH $\cdot$  represent an alkoxy and hydroxyl radical, respectively.



The new alkoxy radical can further propagate the degradation mechanism by reacting with neighbouring hydrogen atoms in several ways. The alkoxy radical can abstract a hydrogen through  $\beta$ -scission of the main chain to produce an aldehyde or it can react with the hydroxyl radical formed in Reaction 4 to produce chain ketones (Gardette et al. 2013). The hydroxyl radical may also react with a neighbouring polymer chain to produce another radical. The carbonyl groups formed during the thermo-oxidative degradation process, such as ketones and aldehydes, are able to absorb visible light and consequently contribute to an increase in yellow colour of the polymer. The yellowing of a polymer is a common characteristic used to evaluate the extent of thermo-oxidative degradation (Allen, Edge, and Hussain 2022).

The termination step involves recombining radical sites, which can either manifest in crosslinking, and/or new non radical products, shown by Reactions 5-7 (Spalding and Chatterjee 2017).



The propagation step is a continuous process which generates an increasing number of radicals, ultimately leading to the degradation of the polymer revealed either through crosslinking, branching and/or chain scission. Although these reactions occur simultaneously, typically one mechanism dominates. Many researchers have found that the degradation pathway is primarily dependent on the polymer type as well as processing conditions to which the polymer is exposed to (C. Chen et al. 2016; Pinheiro, Chinelatto, and Canevarolo 2004; Oliveira, Cramez, and Crawford 1996).

Pinheiro et al. (2004) investigated the competition between chain scission and chain branching of polyethylene processed using a co-rotating twin-screw extruder and determined that generally higher temperatures and shear promote chain scission due to the enhanced mobility of the macromolecular polymer chains, while the reverse conditions resulted in crosslinking. Similar observations were made by Scaffaro et al. (2009) who studied the effect of processing parameters on the formation of chain scission and branching in high density polyethylene. A batch mixer processed polyethylene using various conditions and it was determined that lower temperatures and mixing speeds promoted crosslinking mechanisms due to the limited mobility of macromolecular chains, while the opposite conditions resulted in chain scission (Scaffaro et al. 2009). Due to the zero-shear nature of the rotational molding process, crosslinking and branching

mechanisms are typically the dominant thermo-oxidative degradation reactions (Oliveira, Cramez, and Crawford 1996). However, chain scission can still take place and is usually evident in polymers where heavier substituents are attached to the polymer backbone, creating a more rigid structure susceptible to scission. Thus, polypropylene is more prone to chain scission reactions whereas polyethylene typically favours crosslinking (Kholodovych and Welsh 2007).

### **2.3.1. Chain Scission Reactions**

Thermo-oxidative degradation is manifested in chain scission reactions when the alkoxy ( $\text{RO}\cdot$ ) and peroxy ( $\text{RO}_2\cdot$ ) radicals that arise due to oxygen attacking the polymeric chain proceed to abstract a hydrogen atom from a neighbouring chain, resulting in  $\beta$ -scission with the formation of carbonyl end groups. Such a reaction decreases the polymer's molecular weight and viscosity, resulting in deteriorated polymer properties (Pinheiro, Chinelatto, and Canevarolo 2004).

Klemchuk and Horng (1984) exposed unstabilized HDPE films prepared by compression molding to an oxygen uptake apparatus to study the effects of chain scission caused by thermo-oxidative degradation. It was reported that for every one molecule of polymer, two molecules of oxygen were consumed, and one chain scission took place on average. The chain scissions resulted in a decreased number average molecular weight ( $M_n$ ) and a more substantial reduction in the weight average molecular weight ( $M_w$ ), indicating that larger molecules are more susceptible to chain scissions. Small amounts of chain scissions resulted in a significant reduction in the polymer's elongational properties and both carbonyl and hydroperoxide absorbance increased dramatically (Klemchuk and Horng 1984).

The effects on rheological properties of polypropylene subject to chain scission reactions via multi-pass extrusion was examined by Da Costa et al. (2005). As the processing temperature and number of extrusions increased, a rapid increase of chain scissions of the polypropylene

molecules was observed and it was determined that these scissions occurred close to the center of the macromolecule. The increase in chain scissions resulted in a reduced molecular weight which was demonstrated by an increase in MFI and significant reductions in complex viscosity and elasticity (Da Costa, Ramos, and Rocha 2005).

### **2.3.2. Crosslinking Reactions**

The occurrence of crosslinks and long chain branches (LCB) arise due to the addition of an alkyl radical with another alkyl radical or a carbon-carbon double bond. The resulting effect is an interconnected network of polymer chains whose size and quantity is dependent on the degree of crosslinking. As mentioned in previous sections, crosslinking and chain branching are the dominant thermo-oxidative degradation mechanisms in relatively low shear processes such as in rotational molding. These reactions result in significant changes in rheological and mechanical properties of the polymer.

Dynamic oscillatory rheology performed in the linear viscoelasticity (LVE) region is a commonly used method to detect changes in the polymer's microstructure by evaluating its complex viscosity as well as viscoelastic properties that are sensitive to chain length and the degree of entanglements, namely the storage ( $G'$ ) and loss modulus ( $G''$ ). As the degree of crosslinking increases, the polymer structure undergoes significant alterations, followed by corresponding viscoelastic behaviours. Generally, crosslinking promotes higher  $G'$  values indicating a stiffer material capable of storing more elastic energy, while its effects of  $G''$  can vary (Di et al. 2024). In addition, higher degrees of crosslinking typically result in a higher molecular weight polymer with an increased viscosity and decreased MFI (Mendes, Cunha, and Bernardo 2011; Erbetta et al. 2014). Cuadri et al. (2017) carried out rheological measurements in the LVE region of compression molded high-density polyethylene (HDPE) samples over a range of degradation temperatures and

times. As degradation conditions progressed, so did the formation of crosslinking and LCB, accompanied by greater complex viscosities and storage moduli. These results were ascribed to the decreased mobility of the polymer chains which resulted in an overall stiffer material (Cuadri and Martín-Alfonso 2017).

Crosslinking and LCB reactions have complex effects on the mechanical properties of the polymer which depends on the extent of these reactions. Moderate crosslinking can be beneficial in increasing the impact strength of a material by uniformly distributing stress throughout the polymer and consequently preventing crack propagation (Inoue 1994). However, as the degree of crosslinking increases, an overly rigid structure is formed which weakens the polymer's ability to absorb impact energy and results in excessive brittleness. This was shown by both Oliveira et al. (1996) and Chen et al. (2019) who conducted similar studies investigating impact properties of degraded rotomolded polyethylene, where both studies found that the degraded polymer experienced excessive crosslinking and resulted in brittle failure with a significantly lower impact strength compared to samples where degradation was not evident.

Due to the continuous nature of the propagation step during thermo-oxidative degradation, the degree of crosslinking is often excessive and difficult to control, resulting in detrimental effects on impact properties. However, the incorporation of stabilizers may help minimize the degree of crosslinking and consequently alleviate the damaging effects on mechanical properties.

## **2.4. Role of additives**

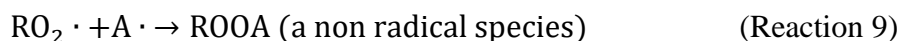
The role of stabilizers as additives in polymer processing is to protect the polymer from the adverse effects of degradation mechanisms that lead to deteriorated physical and mechanical properties. Antioxidants are the main additives used to disrupt the free radical process that arises



during thermo-oxidative degradation and they are typically added in relatively small concentrations ranging between 0.01-0.1 wt% (Carrero et al. 2015). Antioxidants are divided into two categories depending on their chemical pathways: primary antioxidants and secondary antioxidants. A third additive studied is an ultraviolet (UV) stabilizer which is normally used to protect the polymer from photodegradation; however, recent studies have suggested that UV stabilizers can play a role in alleviating thermo-oxidative degradation effects as well.

#### 2.4.1. Primary Antioxidants

Primary antioxidants are commonly referred to as “radical scavengers” and they function by rapidly reacting with peroxy and alkoxy radicals by donating their reactive hydrogen, thereby inhibiting the further propagation of free radicals (Moss and Zweifel 1989). Sterically hindered phenols are the most commonly used primary antioxidant, where large substituents are attached to the phenolic ring distributing the electron cloud better around the whole molecule and thereby stabilizing a free radical drawn away from a polymer, indefinitely. During the reaction with a peroxy radical, the antioxidant is converted to a phenoxy radical ( $A\cdot$ ) while the peroxy macroradical ( $RO_2\cdot$ ) is converted into a hydroperoxide (Reaction 8). Typically, the second and sixth positions of the phenolic antioxidant contain tertiary butyl groups which help provide significant steric hindrance and further shield the newly formed phenoxy radical from the initiation of a new oxidation cycle (Gijssman 2008). The phenoxy radical can also react with a peroxy radical to form a stable, non-radical product (Reaction 9).



Although successful in delaying the onset of degradation and alleviating negative impacts on polymer properties, a main drawback of primary antioxidants is their susceptibility to

discoloration upon oxidation (Spalding and Chatterjee 2017; Sharifi et al. 2012). The phenoxy radical ( $A\cdot$ ) formed during stabilization can undergo resonance to form resonance-stabilized intermediate products. One of these intermediate products are quinone methides which have been revealed by Pospisil et al. (2002) to be the main contributors to polymer discoloration in degraded polyolefins stabilised with phenolic antioxidants. Quinone methides have also been evaluated by Allen et al. (2022) for their ability to absorb visible light and it was determined that these intermediate products are heavily responsible for the increased yellowing in polyolefins where phenolic antioxidants are used. This phenomenon was validated by Sharifi et al. (2012) who determined that the most degraded polyethylene samples subject to multi-pass extrusion prior to rotomolding resulted in less yellowing compared to non-degraded samples containing primary antioxidants. Thus, it was concluded that the appearance of yellowing was mainly due to the transformation products formed by the primary antioxidants while protecting the polymer, rather than due to carbonyl groups formed during the thermo-oxidative degradation process (Sharifi et al. 2012).

#### **2.4.2. Secondary Antioxidants**

Secondary antioxidants are responsible for converting unstable hydroperoxides into non-radical and thermally stable products. Thus, the decomposition of hydroperoxide into reactive alkoxy and hydroxy radicals that occurs during the propagation step of thermo-oxidative degradation is hindered (Sarrabi, Lacrampe, and Krawczak 2015). Secondary antioxidants are rarely used alone since they do not become active until a melt temperature of 180-200°C is reached, thus they are often combined with primary antioxidants to yield synergistic effects and delay the onset of degradation (Cramez, Oliveira, and Crawford 2003; Allen, Edge, and Hussain 2022).

Although secondary antioxidants are not directly explored in this thesis, it is understood that the stabilizer packages in the polyethylene resins received from the supplier contain a mixture of primary and secondary antioxidants.

### **2.4.3. UV Stabilizers**

UV stabilizers such as UV absorbers and hindered amine light stabilizers (HALS) protect the polymer through distinct mechanisms from photodegradation, a type of polymer degradation that arises from exposure to UV radiation; free radical degradation can be initiated by any sufficiently energetic source like high temperatures, gamma radiation or UV radiation, as examples. Although originally intended to be used as a UV stabilizer, in some cases HALS have been proven to provide significant protection against thermo-oxidative degradation in polyolefins (Gugumus 1994). HALS are increasingly being used as long-term heat stabilizers, especially in cases where primary phenolic antioxidants are not suitable due to secondary factors such as discolouration (Gijsman 2017)

The main function of HALS are to scavenge and react with radicals to ultimately convert them into stable products (Spalding and Chatterjee 2017). Although the effects in providing thermo-oxidative stabilization have been observed, the mechanisms driving these effects are far less studied compared to those initiated by UV radiation.

Gugumus (1994) compared the heat stabilization effects of using HALS to protect polypropylene from thermo-oxidative degradation with the effects of a primary antioxidant. It was determined that the deterioration in mechanical properties as a function of time was gradual and steady with samples containing exclusively HALS whereas when only a phenolic antioxidant was used, the mechanical properties were unaffected for a specific amount of time before failing catastrophically after a certain induction period (Gugumus 1994). Gensler et al. (2000) reached a

similar conclusion where HALS-stabilized samples successfully alleviated thermo-oxidative degradation effects on mechanical properties; however, the deterioration was gradual compared to samples containing phenolic antioxidants where catastrophic failure occurred after a specific induction period.

Although HALS has shown promising results when used as a long-term heat stabilizer, there is still no consensus of the mechanism involved and it is thought to be circumstance dependent (Gijsman 2017). Therefore, at the moment, HALS is still predominately used as a UV stabilizer. However, despite not being its intended function, it has been shown to play an important role in alleviating thermo-oxidative degradation effects. Much research is still required to fully understand HALS' role in the stabilization of polyolefins.

## **Chapter 3: Rotomolding Process**

### **3.1. Apparatus and Procedure**

A uniaxial rotational molding machine was used to process powdered resin. The process began with charging a 90 x 90 mm cubic aluminum mold with 100 g of powdered material. The mold, once charged, rotated on a single axis at a constant speed of 4 rotations per minute. Meanwhile, an oven was heated to a predetermined temperature and was placed over the rotating mold. The internal air temperature of the mold was monitored by a mounted thermocouple in the mold's centre. Once the mold reached a desired peak internal air temperature (PIAT), the oven was removed, and a fan was placed directly in front of the mold producing a stream of forced air at 3 m/s. The sample was removed from the mold once the internal air temperature reached 80°C. The final sample resembled a hollow box with its front and back panels missing and an average wall thickness of 3 mm.

### **3.2. Selection of Operating Conditions in Rotomolding**

The selection of a peak internal air temperature (PIAT) during rotational molding will heavily determine the degree of degradation and subsequent physical and mechanical properties of the final part. A PIAT that is too high produces an over-cooked part with evidence of excessive thermo-oxidative degradation, either revealed through a colour change of the material or through significant mechanical losses. On the other hand, too low of a PIAT results in incomplete sintering, with excessive microscopic voids on the surface due to trapped air between the powder particles which will also show significant mechanical losses (Sharifi et al. 2012). Therefore, the optimum PIAT for rotational molding should be selected just prior to the onset of degradation during which the melt viscosity is relatively high, yet processing is still manageable. Additionally, the heating rate of the mold can also affect final product properties where too fast of a heating rate can lead to

incomplete sintering of particles which may compromise the mechanical properties of the final part. On the other hand, too slow of a heating rate leads to longer cycle times in which the polymer is exposed to heat, leading to increased thermo-oxidative degradation (Umbare and Arakerimath 2024). The heating rate of the mold is controlled by the selected oven temperature for the rotomolding process. A higher oven temperature increases the driving force for heat transfer and ultimately increasing the heating rate of the mold.

The selection of a PIAT along with the oven temperature were either selected based on literature findings or based on screening trials outlined in Section 5.3.2., depending on the recycling process studied.

## **Chapter 4: Multi-Pass Extrusion Recycling with HDPE**

### **4.1. Introduction**

A recycling process involving multi-pass extrusion of HDPE will be presented in this chapter; this is a classical research technique for studying recycling. The purpose of multi-pass extrusion is to intentionally consume the stabilizers present and vary the sensitivity of the polymer to subsequent processing indicative of recycling, which in the present case was rotomolding; each pass of a resin through the extruder is intended to make the polymer more sensitive to degradation by rotational molding. The results of physical, mechanical and rheological analyses conducted on the recycled rotomolded samples will be presented along with the discussion of any thermo-oxidative degradation evidence resulting from reprocessing the material. The addition of an antioxidant additive in this recycling process will also be explored and compared with the results from the process without antioxidant in order to investigate its ability to mitigate thermo-oxidative degradation effects on the recycled material.

### **4.2. Materials**

The resin used in this recycling process is a stabilized commercial high-density polyethylene (ExxonMobil™ HD 8660.29) powder supplied by Imperial Oil Ltd; the polymer was referred to as HD 8660.29 in the studies. The particle size averaged around 500 microns. This resin has a melt index of 2.0 g/10min and is known to be highly stabilized with antioxidants and UV stabilizers for rotational molding applications. The supplementary additive explored in this recycling process is Irganox 1010 also known as Pentaerythritol tetrakis(3-(3,5-di-tert-butyl-4-hydroxyphenyl)propionate), a commercially well-known primary antioxidant. This is a sterically hindered primary phenolic antioxidant stabilizer aimed to protect the polymer against thermo-oxidative degradation effects during processing.

## 4.3. Methods

### 4.3.1. Recycling Process

An 18 mm Leistritz MICRO18 Co-Rotating Twin Screw Extruder was used to process the polyethylene powder. As the polymer exited the extruder, it was water cooled and then pelletized into 3 mm pellets. A sample was collected for each pass, while most of the material from a pass was re-fed into the extruder, for up to three additional processing passes to progressively consume the stabilizers present and vary the level of degradation in the polymer. The first time that the material was processed by the extruder was called “Pass 1” and the pass number increased as the material was reprocessed over again for a total of Pass 1-4 materials. A grinding mill (Kinematica Polymix PX-MFC 90D, Switzerland) with a 2.0 mm mesh was used to grind the extruded pellets obtained from Passes 1-4 into powder suitable for rotomolding; an alternate 0.5 mm mesh was not used despite better matching the vendor-supplied particle size because the unit was not cryogenically cooled and the polymer would tend to partially melt due to the more intense milling. The resulting Pass 1-4 powders were each manually blended with fresh virgin HD 8660.29 resin (Pass 0) at 10, 20 and 30 wt% recycled content. These blends were then rotomolded as outlined in Section 3.1 and characterized. The rotomolder was operated using an oven temperature of 300 °C and a PIAT of 215 °C before cooling.

The same recycling process using the extruder was repeated with the addition of 0.1 wt% of Irganox 1010 antioxidant powder, which was dry blended with the extruded pellets before reprocessing the material in the extruder. The Pass 1-4 materials containing 0.1 wt% of Irganox 1010 antioxidant were collected, blended with 30 wt% of fresh virgin HD 8660.29 resin and used for rotomolding. These samples were referred to as Pass 1-4A. A summary of the naming convention for the rotomolded samples studied in this section is outlined in Table 4.1 below.



Table 4.1. Naming convention of rotomolded samples from multi-pass extrusion recycling with HD 8660.29

<b>Resin: HD 8660.29</b>		
<i>Rotomolded Sample Name*</i>	<i>Number of extrusions of HD 8660.29</i>	<i>Irganox 1010 (wt%)</i>
Pass 0	0	0
Pass 1	1	0
Pass 2	2	0
Pass 3	3	0
Pass 4	4	0
Pass 1A	1	0.1
Pass 2A	2	0.1
Pass 3A	3	0.1
Pass 4A	4	0.1

\*A percentage may also be included beside the sample name, indicating the weight percent (wt%) of recycled powder blended with virgin resin.

#### **4.3.2. Melt Flow Index (ASTM D-1238)**

Melt flow index (MFI) as per ASTM D-1238 was used to evaluate changes in polymer viscosity resulting from degradation. A melt flow indexer was used to process extruded pellets taken from each iteration from passing through the extruder (Pass 1-4). An electrically heated barrel was heated to a constant temperature of 190 °C and a 2.16 kg weight was applied to the molten polymer. This weight included the mass of the plunger and an external weight. The mass of the polymer extrudate was weighed after 2-minute time intervals and the MFI, expressed as grams/10 minutes was calculated. Three MFI measurements were conducted for each sample and the average value along with their standard deviations were reported. A larger MFI value signifies lower viscosity while a lower MFI suggests a higher viscosity material.

### 4.3.3. Polymer Sintering Analysis

Polymer sintering occurs during the heating stage of the rotomolding process and involves the coalescence of loosely packed powder particles to form a homogeneous melt in the absence of shear. Trapped air between the powder particles eventually turn into air bubbles during melting which begin to dissolve in the polymer melt as temperature rises. However, the completeness by which the particles fuse during sintering depends on surface tension, resin viscosity, powder properties and particle size (Kontopoulou 1999). Incomplete sintering during the rotational molding process results in air bubbles trapped inside of the polymer melt which yield poor mechanical properties once solidified.

#### *Bubble Dissolution Test*

A bubble dissolution test was performed by use of a Polymer Analysis Vision System (developed in conjunction with Imperial Oil Ltd) where 200 mg of polymer powder was evenly distributed across the surface area of a glass crucible and carefully tamped into place. The polymer powder used for sintering analysis was the same mixture of virgin and recycled powders that would be processed in the rotomolder. The glass crucible containing the polymer powder mixture was placed into a Heat Chamber and luminated from beneath. A microscope charge-coupled device (CCD) camera was used to collect images of the polymer powder during melting and record the number of bubbles present over time. The magnification level of the microscope used was 2x (corresponding to 211-213 pixels per mm). A sintering profile produced by the system recorded the number of bubbles present in the polymer melt approximately every 30 seconds between melt temperatures of 120 °C and 230 °C. The heating rate of the system was approximately 5 °C/min.

### *Surface Void Analysis*

An additional method to evaluate the completeness of sintering during the rotational molding process is by visually inspecting the outer surfaces of the rotomolded parts for the presence of voids.

An image processing software was used to calculate the total percent of void area on the surface of the rotomolded parts. A lubricant containing a mixture of copper and graphite was first rubbed onto a single face of the rotomolded box in order to darken and accentuate the appearance of the void areas. The excess lubricant was wiped away with a wet paper towel. Next, a photo of the lubricated face was taken with a digital camera and uploaded into ImageJ processing software for analysis. The photo was cropped into a 40 mm by 40 mm section taken from the centre of the face and was converted into an 8-bit image while adjusting the image threshold to calculate the void area of the section. The total percentage of sinkhole area on the rotomolded box was estimated by dividing the calculated void area by the area of the cropped section ( $1600 \text{ mm}^2$ ) and multiplying by 100%. A <1% sinkhole area is typically desirable. An example of a 40 mm by 40 mm lubricated section of a rotomolded part with 0.5% and 5.2% void areas are shown in Figure 4.1 A and B below, respectively.

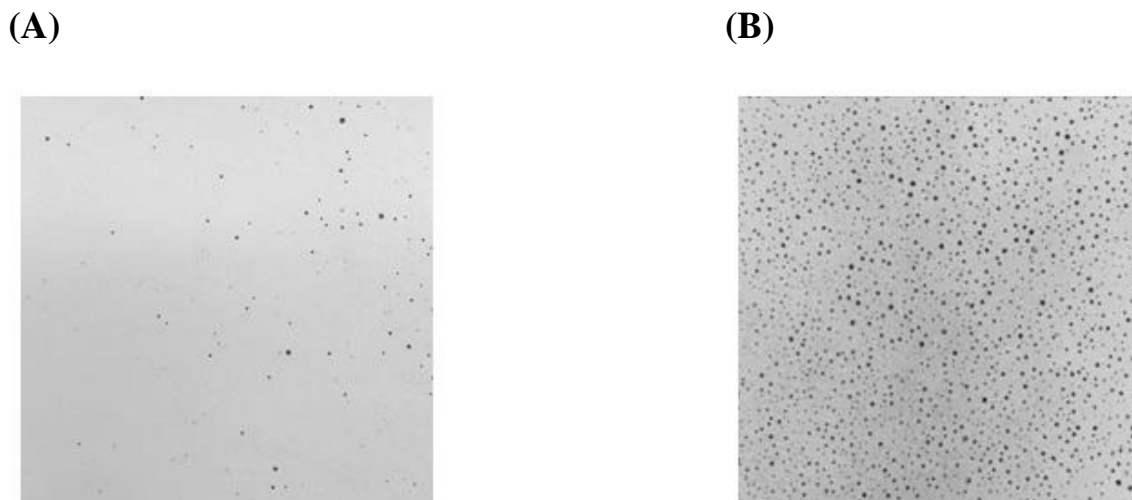


Figure 4.1. A cropped image of the surface of a rotomolded sample containing (A) 0.5% void area and (B) 5.2% void area

#### **4.3.4. Izod Impact Test (notched) ASTM D256, ISO 180**

A Zwick/Roell HIT25P Pro Pendulum impact tester was used to carry out a notched Izod Impact Test as per ASTM D256, ISO 180 to assess the impact strength of the recycled rotationally molded boxes; this method was chosen over dart impact testing so that more samples could be generated per molded box. An Izod Impact test calculates the energy absorbed by a specimen when it is struck by a swinging pendulum. The pendulum is initially raised to a specific height while the specimen is clamped into place in a test fixture. Once the pendulum is released from its initial height, its potential energy is converted to kinetic energy which is then absorbed by the specimen upon impact. The amount of energy absorbed by the specimen can be determined based on the height to which the pendulum swings after striking the specimen. A higher value of Izod impact strength signifies greater toughness indicating that the polymer can deform plastically without fracturing.

The specimens used for the Izod impact test were obtained by carefully cutting a face of the rotomolded box into rectangular test specimens with dimensions of approximately 64 x 13 x 3 mm. Specimens were notched using a Mastercraft router table notching apparatus and were placed

inside of a freezer and allowed to cool to -40 °C for at least 24 hours prior to testing. A pendulum corresponding to 5.5 J was selected for testing. Five specimens were tested for each rotomolded box and the average value was reported along with the standard deviation.

## **4.4. Results and Discussion**

### **4.4.1. Melt Flow Index Results**

The MFI of the extruded pellets (prior to rotomolding) with and without the addition of 0.1 wt% Irganox 1010 antioxidant was investigated and compared to the MFI of the unprocessed virgin HD 8660.29 (Pass 0) powder in order to evaluate changes in polymer viscosity. The results are shown in Figure 4.2. The MFI for all passes through the extruder was lower compared to the virgin HD 8660.29 powder (Pass 0), with the Pass 4 material exhibiting the most significant decrease in MFI. The decreasing MFI indicates a higher viscosity material produced in the extruder due to crosslinking and branching within the polymer, leading to longer chains and an overall restriction in molecular movement.

The addition of antioxidant only showed a notable difference in the Pass 4 material which displayed a higher MFI, suggesting that the antioxidant was helpful in preventing some crosslinking from occurring while subjected to high heat and mechanical stresses in the extruder.

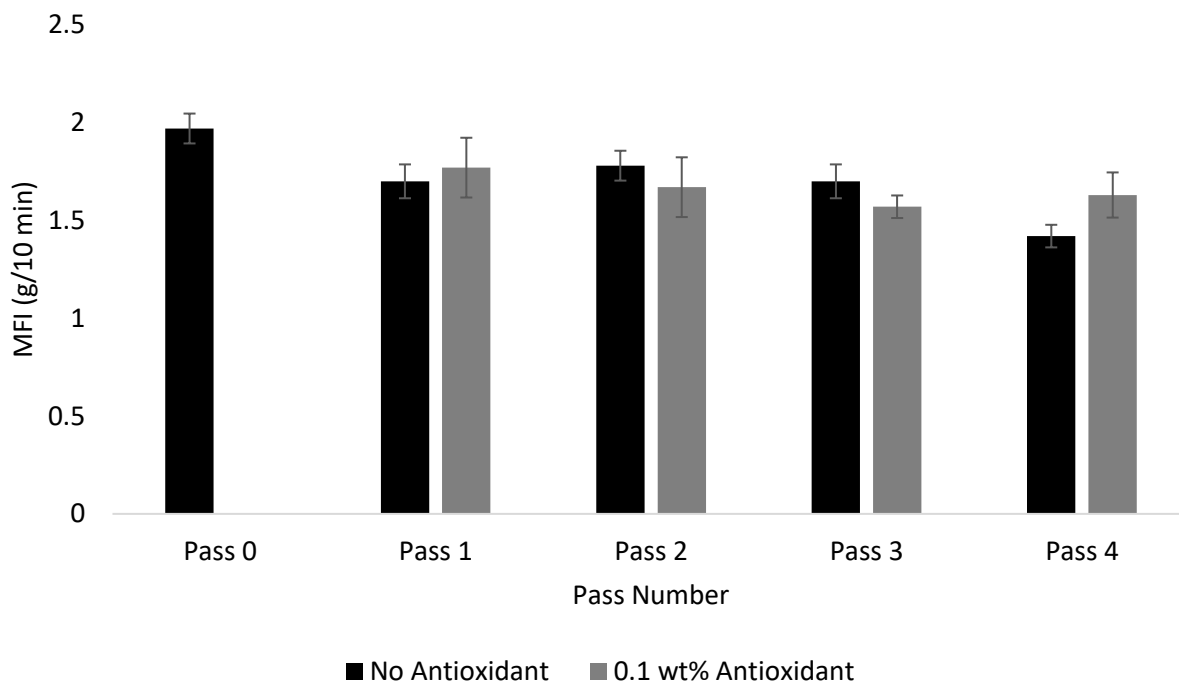


Figure 4.2. MFI for Pass 1-4 extruded HD 8660.29 material with and without the addition of a supplementary antioxidant compared with unprocessed (Pass 0) HD 8660.29 powder

#### 4.4.2. Results of Polymer Sintering

A bubble dissolution test was performed for Passes 2 and 4 powder blended with 30% recycled content prior to rotomolding in order to evaluate the progression of bubbles within the polymer melt as temperature increased and to relate the results to the powder's sintering behavior in the rotomolder. The number of bubbles in the polymer samples with and without the addition of 0.1 wt% Irganox 1010 antioxidant are shown in Figures 4.3 and 4.4, respectively. Ideally, curves should approach zero visible bubbles for a temperature above the melting point of the polymer but not so high that the polymer degrades.

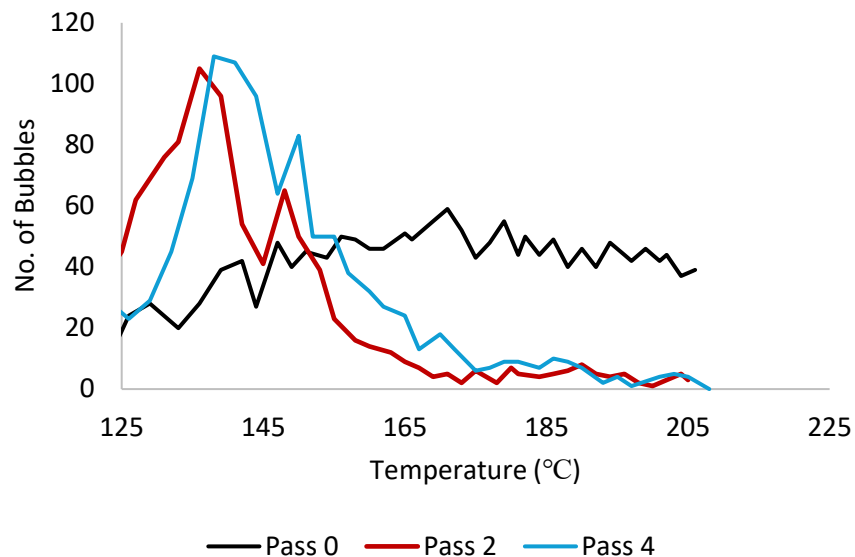


Figure 2.3. Number of bubbles in the polymer melt plotted with temperature for Pass 2 and Pass 4 HD 8660.29 powders with 30% recycled content compared with unprocessed virgin HD 8660.29 (Pass 0)

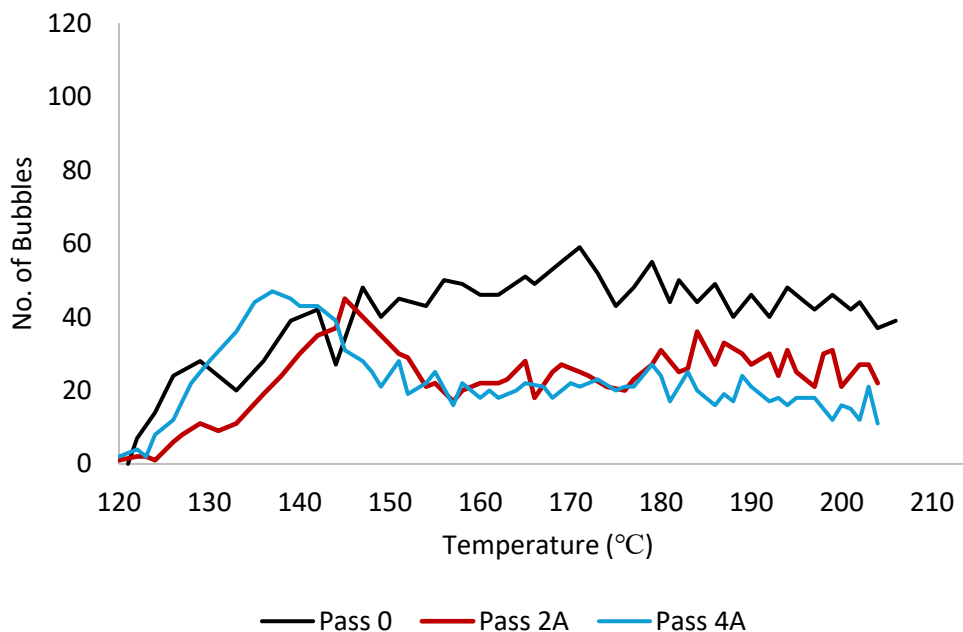


Figure 4.4. Number of bubbles in the polymer melt plotted with temperature for Pass 2A and Pass 4A HD 8660.29 powders with 30% recycled content compared with unprocessed virgin HD 8660.29 (Pass 0)

Figure 4.3 shows that Passes 2 and 4 without antioxidant were able to reach nearly zero bubbles near the ending temperature (around 180 °C) despite initially having a significantly higher number of bubbles at the starting temperature (around 130 °C), indicating complete sintering of the polymer powder. The addition of the primary antioxidant initially suppressed the number of bubbles formed between temperatures of 125-150 °C and the overall sintering behaviour more closely resembled that of the virgin HD 8660.29 polymer; however, the powders never achieved zero bubbles at the end temperature, and instead fluctuated around 20 bubbles as shown in Figure 4.4. Polymer sintering depends on surface tension, resin viscosity, powder properties and particle size, and given that the powder properties and particle size were unchanged between samples, this discrepancy in sintering was either attributed to surface tension or resin viscosity. The MFI results revealed an overall higher viscosity for the Pass 2 and 4 samples (as discussed in Section 4.4.1), which typically results in worse particle sintering, a condition not detected by the bubble dissolution test. Thus, it is possible that the addition of antioxidant lowered the surface tension of the polymer particles due to an excessive amount of antioxidants accumulating on their surfaces, thus decreasing the driving force for particle coalescence. The virgin HD 8660.29 resin is known to contain a relatively high stabilizer content which may explain why the virgin powder exhibited a larger number of bubbles in the polymer melt compared to the recycled powders (shown in Figure 4.3) since Pass 2 and 4 powders experienced a reduction in stabilizer content during multiple passes in the extruder.

The voids on the surfaces of the rotationally molded parts obtained from Passes 1-4 at 10%, 20% and 30% recycled content were examined and compared with the unrecycled HD 8660.29 (Pass 0) rotomolded part, shown in Figure 4.5. The void area on the surface of the rotomolded part for Pass 0 was less than 1% which is typically desired in the rotomolding industry and indicates



strong, well fused parts. Void area increased with each successive pass number, indicating difficulties in particle sintering at the mold wall during rotomolding. This is likely due to crosslinking in the polymer's microstructure which leads to resistance to flow during melting, and ultimately hindering uniform sintering.

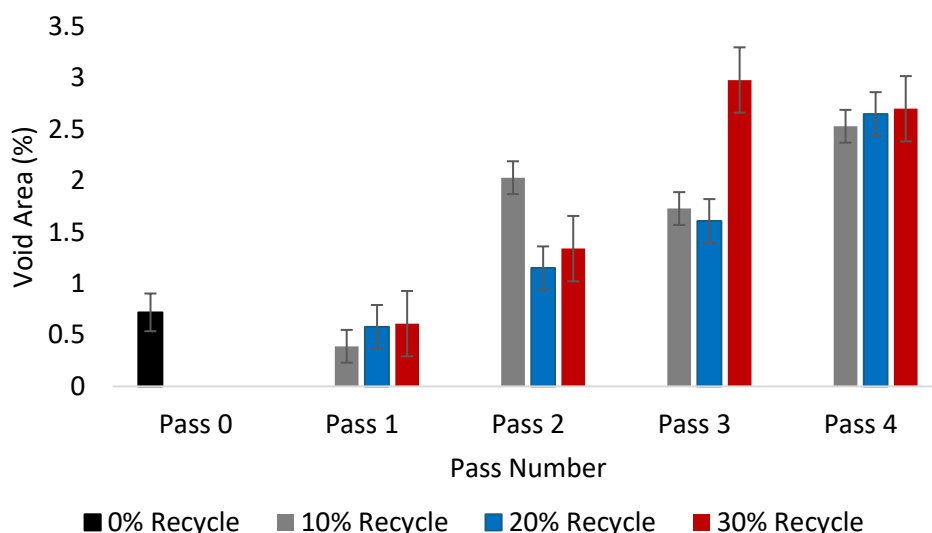


Figure 4.5. Percentage of void area on the surface of the rotationally molded boxes from Passes 1-4 HD 8660.29 with 10, 20 and 30% recycled content compared with virgin HD 8660.29 (Pass 0)

The surface voids on rotomolded samples, Pass 2 and Pass 4 were compared with their respective samples containing 0.1% Irganox 1010 antioxidant, Pass 2A and Pass 4A, shown in Figures 4.6 and 4.7, respectively. The addition of 0.1% Irganox 1010 antioxidant displayed an even higher percent void area when compared to the samples without antioxidant indicating poorer sintering of particles at the mold wall during rotomolding. This behaviour corresponds to the difficulties in sintering during polymer melting revealed in the bubble dissolution test with powder samples containing antioxidant. Since the virgin HD 8660.29 is known to already be stabilized with antioxidants, the overall deterioration of sintering capability shown by the samples containing additional Irganox 1010 antioxidant may be attributed to an overabundance of antioxidants.

Specifically, when excessive antioxidants are incorporated in a polymer powder, they can accumulate on the particle's surface, reducing the cohesive forces and surface tension that are necessary for adequate sintering.

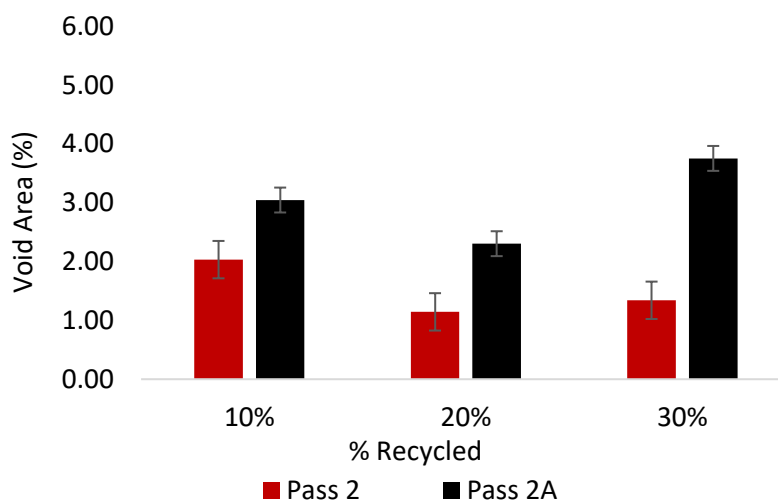


Figure 4.6. Percentage of void area on the surface of HD 8660.29 rotomolded samples without antioxidant (Pass 2) and with the addition of antioxidant (Pass 2A) for 10, 20 and 30% recycled content

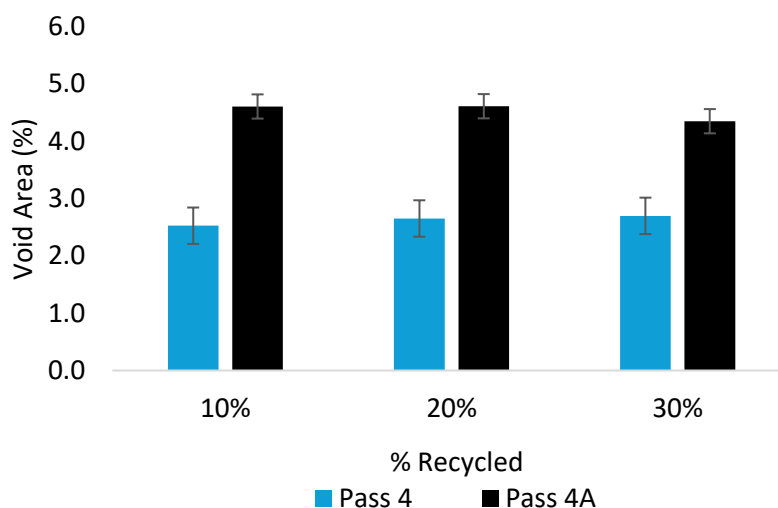


Figure 4.7. Percentage of void area on the surface of HD 8660.29 rotomolded samples without antioxidant (Pass 4) and with the addition of antioxidant (Pass 4A) for 10, 20 and 30% recycled content

#### 4.4.3. Impact Test Results

A notched Izod impact test was conducted on rotomolded samples that were processed using Pass 1-4 extruded polymer with 10, 20 and 30 wt% recycled content and the results are shown in Figure 4.8. The impact strength for Pass 1-4 materials at all recycled percentages fluctuated heavily around an average value of about 20 kJ/m<sup>2</sup>. Given that the rotomolded sample containing 100% virgin HD 8660.29 polymer (Pass 0) had an impact strength of around 17 kJ/m<sup>2</sup>, the degradation resulting from multi-pass extrusion of HD 8660.29 did not result in significant mechanical losses. Although it was revealed through MFI that increasing passes resulted in higher viscosities due to crosslinking, it is possible that the stabilizers present in the resin were sufficient to combat excessive crosslinking during multiple extrusion passes which would otherwise result in a significant loss in mechanical properties of the polymer.

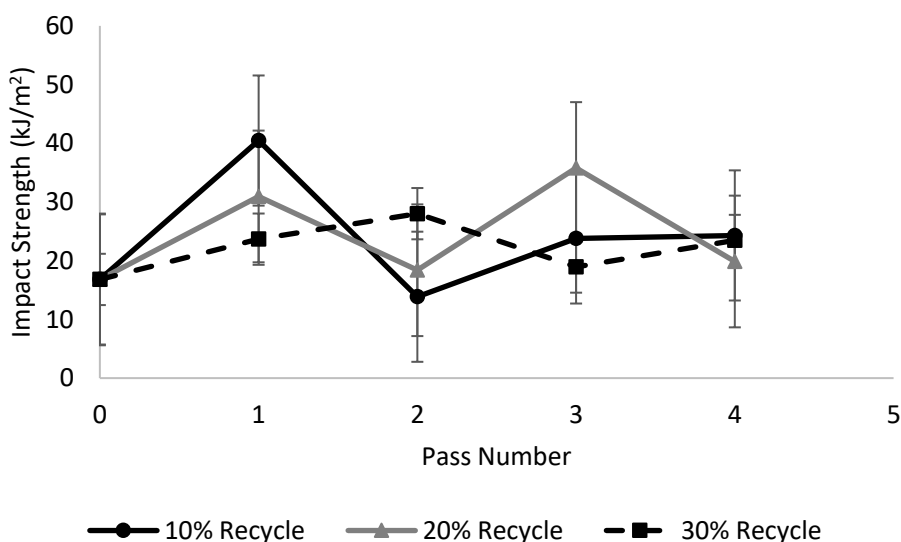


Figure 4.8. Izod impact strength for notched rotomolded samples processed using Pass 1-4 HD 8660.29 extruded material with 10, 20 and 30 wt% recycled content

The impact strength of Pass 2 and 4 rotomolded material were compared with Pass 2A and 4A material, shown in Figures 4.9 and 4.10, respectively. No significant changes in impact strength

with the addition of Irganox 1010 antioxidant were observed for the Pass 2 and 4 rotomolded samples. This may be due the virgin HD 8660.29 resin already being heavily stabilized, so the incorporation of an additional antioxidant had minimal impact on mechanical properties.

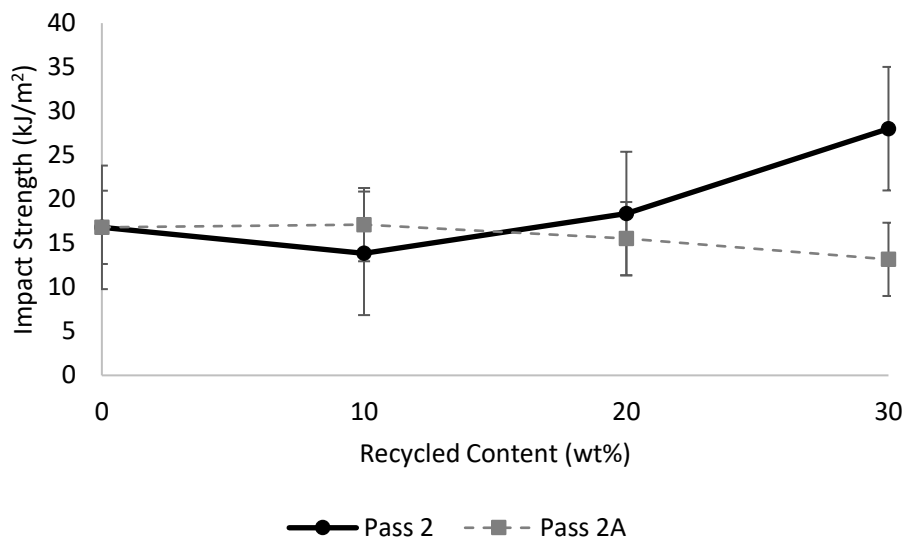


Figure 4.9. Impact strength of Pass 2 HD 8660.29 rotomolded material with and without the addition of Irganox 1010 antioxidant

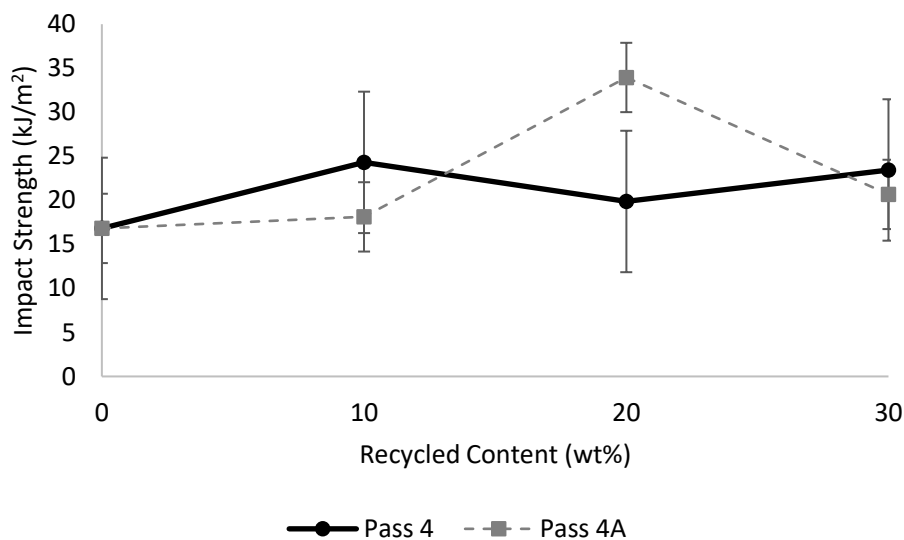


Figure 4.10. Impact strength of Pass 4 HD 8660.29 rotomolded material with and without the addition of Irganox 1010 antioxidant

## 4.5. Conclusions

Overall, the HD 8660.29 polymer subject to a multi-pass extrusion recycling process resulted in minimal changes to polymer properties. It was revealed through MFI that increasing passes through the extruder did in fact alter the molecular structure of the polymer, causing crosslinking and/or LCB shown by a slight increase polymer viscosity. However, the strong sintering ability and minimal changes in impact strength displayed by the recycled samples (Pass 1-4) suggest that the stabilizers present in the HD 8660.29 polymer were sufficient to combat excessive crosslinking which would otherwise result dramatic mechanical losses. The incorporation of a supplementary antioxidant did not show significant changes in impact strength, and resulted in poorer sintering ability which was attributed to an overly stabilized material where excess antioxidant altered the surface chemistry of the particles and effectively hindered particle coalescence. This abundance of antioxidants further proves that the stabilizers present in the virgin HD 8660.29 resin were adequate to avoid depletion during the multi-pass extrusion recycling process, which also explains the minimal deterioration in mechanical and physical properties observed with the recycled samples. Although these results may suggest that recycling did not negatively impact final rotomolded product quality, it is important to note that multi-pass extrusion does not fully capture the reality of PIR with rotomolders. During extrusion, the polymer is subject to high temperatures and mechanical stresses for a very short amount of time (approx. 2 min) compared to rotomolding which is a stress-free process and has a heating cycle approximately 20 min long. While both processes promote thermo-oxidative degradation, the extent of these mechanisms along with their effects on polymer properties cannot be considered identical due to their varying conditions. Thus, a more accurate recycling process of PIR during rotomolding is investigated in the following chapter (Chapter 5).

## **Chapter 5: Multi-Step Granulation Recycling with LLDPE**

### **5.1. Introduction**

A recycling process involving multi-step granulation of rotomolded LLDPE samples will be presented in this chapter. This is a more conventional recycling method aimed to simulate a more accurate post-industrial recycling procedure in which polymer waste from rotomolding is re-integrated in the rotomolding process multiple times; the method allows researchers to better draw conclusions on the role of degradation during rotomolding compared to the multi-pass method of Chapter 4. Since the HD 8660.29 resin explored in Chapter 4 did not demonstrate dramatic changes in polymer properties with repeated recycling, a LLDPE resin with stabilizers formulated for a different application other than rotomolding will be used in this chapter with the aim to highlight the impact of degradation during recycling and gain better insight on the effects that it has on final polymer properties. The results of physical, mechanical and rheological analyses conducted on the recycled rotomolded samples will be presented along with the discussion of evidence of degradation resulting from recycling the material.

### **5.2. Materials**

The resin used for this recycling study is a linear low density polyethylene (ExxonMobil™ LL 8555.25) supplied by Imperial Oil Ltd. whose structure is comprised of short chain branching, denoted as LL 8555.25 in the rest of the chapter. This resin has a melt index of 6.8 g/10 min and according to the vendor it has different stabilizers than that of HD 8660.29, studied in Chapter 4; the resin has a lower viscosity as well compared to HD 8660.29. The supplied resin particle size was nominally between 400-500 microns.

## 5.3. Methods

### 5.3.1. Recycling Process

The recycling process began by directly rotomolding the powdered LL 8555.25 resin as outlined in Section 3.1, grinding it up, then rotomolding again. An oven temperature of 290 °C and a PIAT of 235 °C were used for the rotomolding process. Two faces of a rotomolded box were set aside for characterization while the remaining material was used in the recycling process. The material for recycling was first fed into a plastic granulator which produced polymer pellets averaging 3 mm in size. The pellets were then ground into a powder via a grinding mill (Kinematica Polymix PX-MFC 90D, Switzerland) with a 0.5 mm sieve. A cooling fan producing a stream of forced air at 3 m/s was placed directly in front of the grinding mill to avoid partial melting of the powder during grinding. A mixture of 10 g of ground powder and 90 g of fresh virgin LL 8555.25 powdered resin was manually blended before charging the mold and repeating the rotational molding process. The resulting rotomolded sample was described as “Regrind 1, 10%”. Two faces of the “Regrind 1, 10%” box were set aside for characterization while the remaining material was fed through the plastic granulator, and subsequently the grinding mill to obtain a powder. Again, 10 g of the ground powder was manually blended with 90 g of virgin LL 8555.25 powder before repeating the rotomolding process to obtain a sample described as “Regrind 2, 10%”. This process was repeated twice more to obtain samples described as “Regrind 3, 10%” and “Regrind 4, 10%”.

The entire recycling process was repeated twice more using 30% recycled content and 50% recycled content. These processes produced samples described as “Regrind 1-4 30%” as well as “Regrind 1-4, 50%”. A summary of the naming convention used for rotomolded samples in this chapter is outlined in Table 5.1.

Table 5.1. Rotomolded sample naming convention in multi-step granulation recycling with LL 8555.25

<b>Resin: LL 8555.25</b>	
<i>Rotomolded Sample Name*</i>	<i>Number of times rotomolded LL 8555.25 was ground before reprocessing</i>
Regrind 0	0
Regrind 1	1
Regrind 2	2
Regrind 3	3
Regrind 4	4

\*A percentage may also be included beside the sample name, indicating the weight percent (wt%) of recycled powder blended with virgin resin.

### 5.3.2. Determining Rotomolding Operating Conditions

A PIAT and oven temperature for the rotomolding process with LL 8555.25 were selected based on testing to find an optimal combination by which the recycling study should be conducted; this optimization had not been necessary for HD 8660.29 because earlier researchers had already determined the ideal PIAT and oven temperature. The optimal conditions for which the recycling study was conducted was based on maximizing mean failure energy (MFE) via a dart impact test while minimizing void area. The surface void analysis was conducted to qualify the appearance of a molded box while simultaneously inferring the likelihood of bubbles still present in the mold wall. The percentage of void area on the outer surface of rotomolded boxes with PIATs ranging from 205-235 °C as well as oven temperatures of 290 °C or 300 °C, are shown in Figure 5.1. The MFE via a dart impact test was also determined for the same rotomolded samples, shown in Figure 5.2 below.



As seen in Figure 5.1, as the PIAT increases from 205 °C to 235 °C, the percentage of void area steadily decreased for both oven temperatures. This is due to the general idea that air bubbles formed during melting begin to physically dissolve in the polymer as the temperature increases (Kontopoulou 1999). Figure 5.2 shows a general increase in MFE as PIAT increases for both oven temperatures. This is due to the rotomolded parts being more properly fused at these higher temperatures, resulting in higher impact strengths. However, a PIAT that is too high results in the polymer remaining inside the oven for too long, leading to increased chances of degradation and a corresponding loss in impact strength. Therefore, the optimal conditions selected based on the surface void analysis and MFE were a peak temperature of 235 °C and an oven temperature of 290 °C.

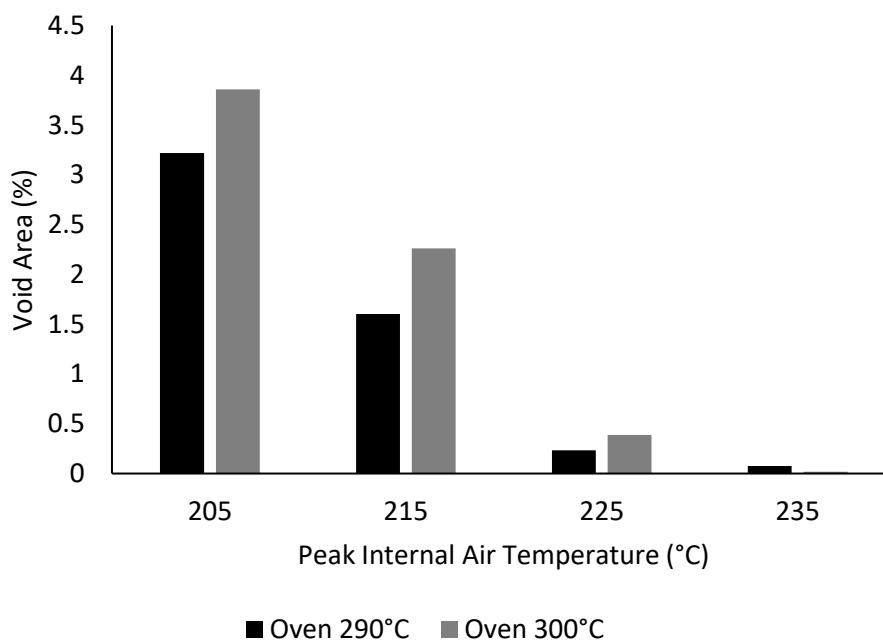


Figure 5.1. Surface void area of LL 8555.25 rotomolded samples with various PIATs and oven temperatures

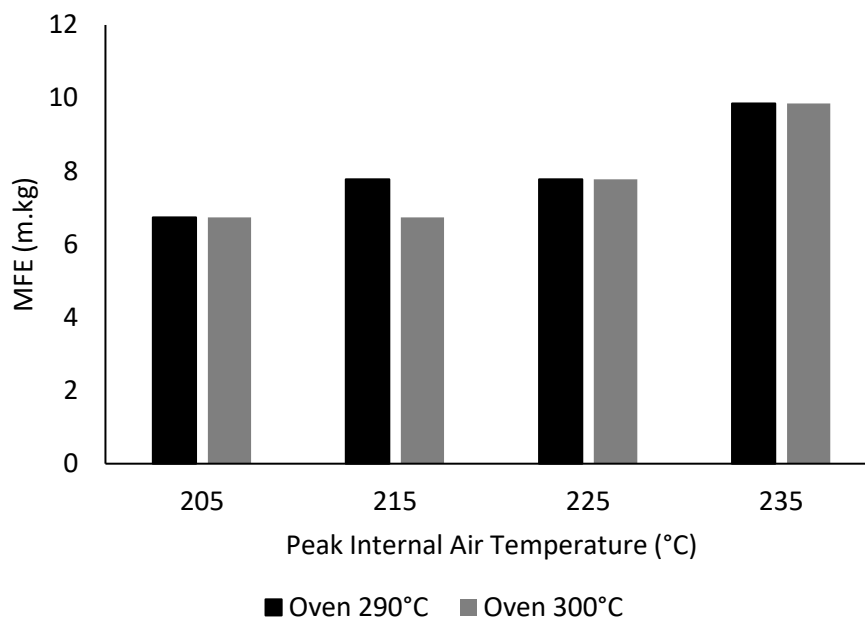


Figure 5.2. MFE of LL 8555.25 rotomolded samples with various PIATs and oven temperatures

### 5.3.3. Dart Impact Test (ASTM D5628)

A Dart Impact Test determines impact resistance by using a free-falling dart to strike a flat, rigid plastic specimen; it is the more typical test used by the rotational molding industry for quality assurance though it requires larger specimens than the Izod test and is more difficult to use for thin-walled specimens. The dart has a fixed weight and is dropped onto the specimen at varying heights. Given the specific mass and height of the dart, this procedure can calculate the energy at which 50% of the specimens will fail upon impact, also known as the mean failure energy (MFE). The technique to calculate MFE is commonly known as the Bruceton Staircase Method or the Up-and-Down Method.

For each test, a rotomolded box was cut into 4 equally sized flat square specimens, with dimensions of 9 cm x 9 cm x 3 mm, taken directly from the peripheral walls of the box. The specimens were cooled to -40°C by placing them in an air circulated freezer for at least 24 h prior to testing. The square specimen was then placed in the test holder with the inner surface of part

facing downwards. Using the Bruceton Staircase Method, a dart with a mass of 6.8 kg (15 lbs) was dropped from an initial height of 0.76 m directly onto the specimen. If the specimen showed signs of failure at the dart's current height, the dart was then lowered by 0.15 m and dropped on the subsequent specimen. Alternatively, if the specimen did not fail at the dart's current height, then the dart was raised by the same increment. This was repeated for all four specimens of the test.

There are several types of failures that may occur during testing. (i) cracks that puncture the entire thickness of the sample, (ii) brittle shatter in which the specimen is broken into several pieces, and (iii) ductile fracture where the specimen is pierced by a dull tear.

The mean failure energy was calculated from Equation 5.1:

$$MFE = hw \quad (\text{Equation 5.1})$$

where,

$h$ : mean-failure height (ft)

$w$ : Dart mass (lb)

And  $h$  can be calculated from Equation 5.2:

$$h = h_o + d_h \left( \frac{A}{N} \pm 0.5 \right) \quad (\text{Equation 5.2})$$

where,

$N$ = Total number of failures or non-failures, whichever is smaller. Also known as “events”

$h_o$ = lowest height at which an event occurred (ft)

$d_h$ = Increment of dart height (ft)

Also,  $A = \sum_{i=0}^k i n_i$

$i = 0, 1, 2 \dots k$  (counting index, starts at  $h_o$ )

$n_i$ = number of events that occurred at  $h_i$ :

Which can be calculated from Equation 5.3.

$$h_i = h_o + id_h \quad (\text{Equation 5.3})$$

The units for MFE were converted from ft.lb to m.kg for all tests.

The dart impact test was used to calculate MFE only for non-recycled rotomolded boxes as well as Regrind 4 boxes since the Regrind 4 material did not have to be ground up to make any additional Regrind samples, thus there was leftover material available for testing; due to the long times to generate sufficient ground regrind content for each subsequent molding experiment, and the amount of material from each rotomolding step required for dart impact testing, this test could only be used in a very limited way. Consider that the calculation for MFE requires at least 1 failure and 1 non failure to compute a value, and since only four specimens were available from a molded box for each test, there was a possibility of being unable to calculate MFE. Typically, when this occurs, the initial height of the dart may be adjusted, and the test can be repeated. However, in the case of recycled boxes, this method was impractical and inefficient for determining the impact strength since there was a good possibility that a failure of calculate the value would mean for a box like Regrind 3 that the whole experimental cycle would have to start again from Regrind 1 to reproduce a new Regrind 3 box for impact testing. It was for this reason primarily that the Izod impact tester was used to calculate impact strength for the recycled rotationally molded boxes.

#### **5.3.4. Izod Impact (Unnotched) Test ASTM D4812, ISO 180**

A Zwick/Roell HIT25P Pro Pendulum impact tester was used to carry out an unnotched Izod Impact Test as per ASTM D4812, ISO 180 to assess the impact strength of the recycled rotationally molded boxes.

The protocol for the Izod impact test was conducted the same as outlined in Section 4.3.4.

An unnotched Izod Impact test was chosen over a notched test since it provides a measure of a materials bulk impact resistance without being influenced by the geometry of the notch.

Moreover, unlike notched tests which only consider the energy required to propagate a crack, the energy absorbed by an unnotched specimen considers both crack initiation as well as propagation, which allows for comparison with the dart impact test. Unnotched specimens typically do not fracture upon impact, however in some cases, such as in heavily degraded polymers, the specimen may either exhibit a ductile fracture or a brittle fracture. A ductile fracture consists of noticeable bending or stretching of the material before breaking which indicates good impact resistance whereas a brittle fracture consists of a sudden break with no prior deformation, common in excessively crosslinked polymers.

#### **5.3.5. Polymer Sintering Analysis**

A polymer sintering analysis was conducted using a bubble dissolution test as well as a surface void analysis as outlined in Section 4.3.3.

#### **5.3.6. Yellowness Index (ASTM D-1925)**

A standard method for calculating the yellowness index (YI) of plastics as per ASTM D-1925 was used to calculate the yellowness of the rotationally molded boxes. This method uses tristimulus values obtained from a colour sensor to compare the magnitude of yellowness to a magnesium oxide standard.

Samples for testing were obtained from the same specimens used for Izod impact testing with dimensions of approximately 64 x 13 x 3 mm taken directly from a face of a rotomolded box. The yellowness is a function of thickness so data comparison was made between specimens of comparable thicknesses. A total of 3 specimens were used to calculate the YI for a sample and their averages and standard deviations were reported.

A Nix Mini 3 portable colour sensor was placed on top of an individual specimen, corresponding to the outer surface of the rotomolded box, and was then fully enclosed with a

cardboard box to prevent any external light from penetrating. The sensor calculated tristimulus values,  $X_{CIE}$ ,  $Y_{CIE}$  and  $Z_{CIE}$  of the specimen which were used in the following YI Equation 5.4:

$$YI = \frac{100(1.28X_{CIE} - 1.06Z_{CIE})}{Y_{CIE}} \quad (\text{Equation 5.4})$$

where  $X_{CIE}$ ,  $Y_{CIE}$  and  $Z_{CIE}$  are the tristimulus values for red, green and blue respectively. A positive YI value indicates the presence and degree of yellowing, whereas a negative value indicates a bluish appearance in the material.

### 5.3.7. Rheological Analysis

Rheology is an effective tool in detecting degradation mechanisms due to its sensitivity to changes in the molecular structure of a polymer melt (Filippone et al. 2015). Particularly, dynamic oscillatory rheology performed at low frequencies in the linear viscoelastic region (LVR) is one of the most effective methods in discriminating among different degradation mechanisms since the strains applied to the polymer are small enough to not damage the polymer's internal structure (Shangguan et al. 2010).

A Discovery HR-2 Hybrid rheometer equipped with 25 mm diameter parallel plates was used to assess rheological measurements of the rotomolded material. All experiments were carried out under air atmosphere. The samples used for testing were taken from 30 mm specimens that were cut directly from the rotomolded boxes.

A Dynamic Strain sweep test was first conducted to determine the LVR of the polymer using a constant frequency of 10 rad/s, a temperature of 215 °C and strain rates ranging from 0.01-100%. A strain rate of 5% was determined to be in the LVR and thus used for all experiments.

A frequency sweep was conducted on the samples using an angular frequency ( $\omega$ ) range of 0.1-100 rad/s and a temperature of 215 °C. This test gave valuable information of the viscoelastic properties of the material such as the storage modulus ( $G'$ ), the loss modulus ( $G''$ ) and the complex viscosity ( $\eta^*$ ). The storage modulus is a measure of the polymer's elastic component while the loss modulus is a measure of the polymer's viscous component. Complex viscosity gives insight on the materials resistance to flow when subjected to an oscillating stress.

## **5.4. Results and Discussion**

### **5.4.1. Results of Polymer Sintering**

#### *Bubble Dissolution Test*

A bubble dissolution test was performed on Regrind 1-4 powders with 30% recycled content prior to rotomolding and compared with virgin LL 8555.25 resin (Regrind 0) in order to evaluate the progression of bubbles within the polymer melt as temperature increased and to relate the results to the powder's sintering behavior in the rotomolder. The results are shown in Figure 5.3. The virgin LL 8555.25 polymer powder began with approximately 60 bubbles at the starting melt temperature of 130 °C. As temperature increased, the number of bubbles steadily decreased until zero bubbles were present, implying complete sintering of the powder is possible at approximately 190 °C. As the Regrind number increased, the number of bubbles generally increased and never reached a completely sintered state as previously seen with the virgin LL 8555.25 powder. As degradation occurs, it is expected that generated crosslinks and branches will increase the viscosity, which would lead to difficulties in complete bubble dissolution during sintering and ultimately result in a larger number of retained bubbles in a molded part.

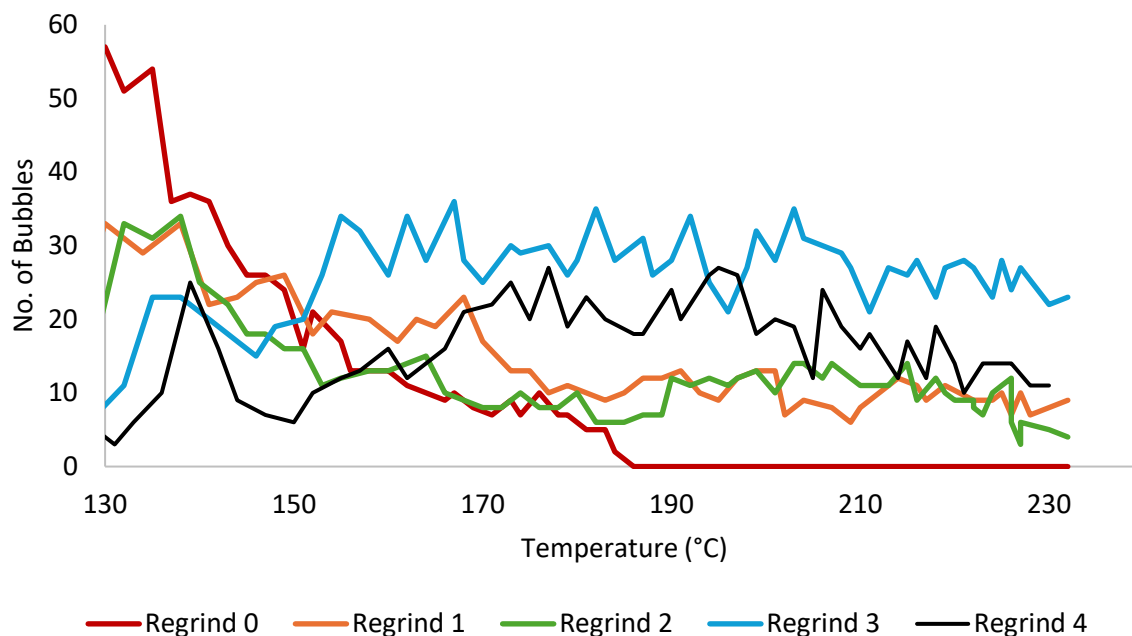


Figure 5.3. Number of bubbles in the polymer melt plotted with temperature for Regrind 1-4 LL 8555.25 powdered material with 30% recycled content compared with virgin LL 8555.25 (Regrind 0)

To consider the impact of recycled content on sintering, a bubble dissolution test was also conducted with Regrind 3 material containing 50% recycled content, which was compared with that of 30% recycled content, as shown in Figure 5.4. The 50% recycled content showed very similar behaviour in the number of bubbles retained in the polymer melt compared to the 30% recycled material implying that increasing the percentage of recycled content does not have a dramatic effect on the powder's sintering ability.



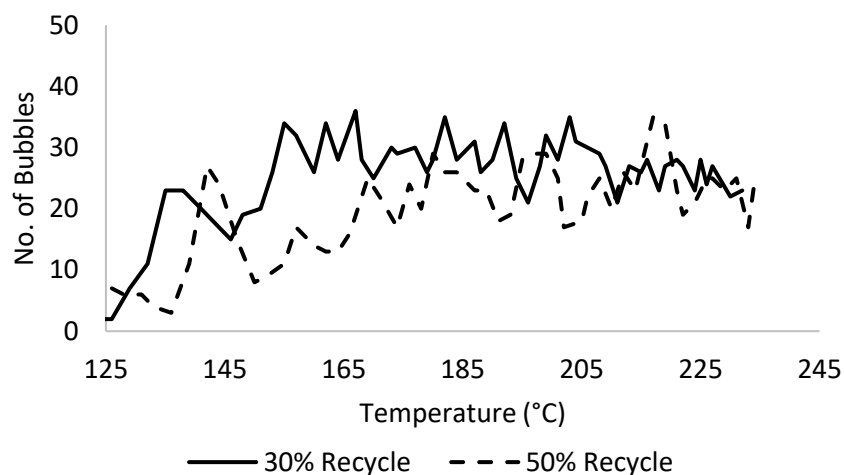


Figure 5.4. Number of bubbles in the polymer melt plotted with temperature for Regrind 3 LL 8555.25 powder containing 30 and 50% recycled content

#### *Surface Void Analysis*

A surface void analysis was performed on Regrind 1-4 boxes with 10%, 30% and 50% recycled content and all were compared against a sample rotomolded box made of the virgin LL 8555.25 resin (Regrind 0), as shown in Figure 5.5. All rotomolded boxes displayed very little to no voids on their outer surfaces implying complete sintering of the particles during rotomolding. No trends could be interpreted from these results since this low void area differed at most by one bubble in the wall of a sample, meaning that all Regrind 1-4 boxes were considered equivalent. It is expected that particles will sinter better at the mold wall compared to the box interior due to the direct heat transfer from the mold which promotes earlier melting and longer times to coalesce the particles present. Additionally, as the mold rotates, the particles along the molds surface experience some compaction from the rotating particle layers above, promoting a better surface finish with less air pockets during melting. This may be why the surface void analysis suggests complete sintering of the particles for all samples while the bubble dissolution test does not.

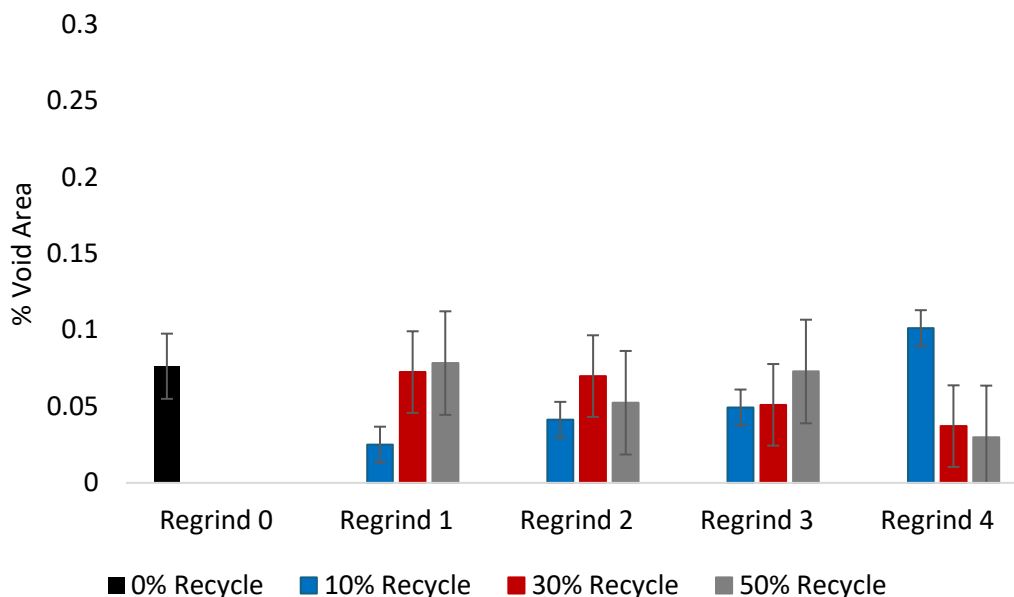


Figure 5.5. Percentage of void area on the surface of the LL 8555.25 rotationally molded boxes from Regrind 1-4 with 10, 30 and 50% recycled content compared with virgin LL 8555.25 (Pass 0)

#### 5.4.2. Results of Impact Tests

##### *Izod Impact Test*

The Izod impact strength was reported for unnotched specimens taken from Regrind 1-4 boxes with 10%, 30% and 50% recycled content and compared with the virgin LL 8555.25, shown in Figure 5.6. A lower impact strength is possible with increasing recycled content as well as increasing Regrind number since polymer degradation seemed evident in the bubble dissolution test. However, Figure 5.6 shows that increasing recycled content as well as regrind number, did not have a dramatic effect on impact strength until Regrind 4 where the strength decreased for all recycled percentages compared to the virgin resin. There is little difference in impact strength when comparing different recycled content in the samples, aside from for Regrind 3 material,

where samples containing 30 and 50% recycled content exhibited a higher impact strength compared to Re grind 3, 10%. This may be due to small amounts of crosslinking (without gelation) or branching improving mechanical strength, which was further investigated through the dart impact test.

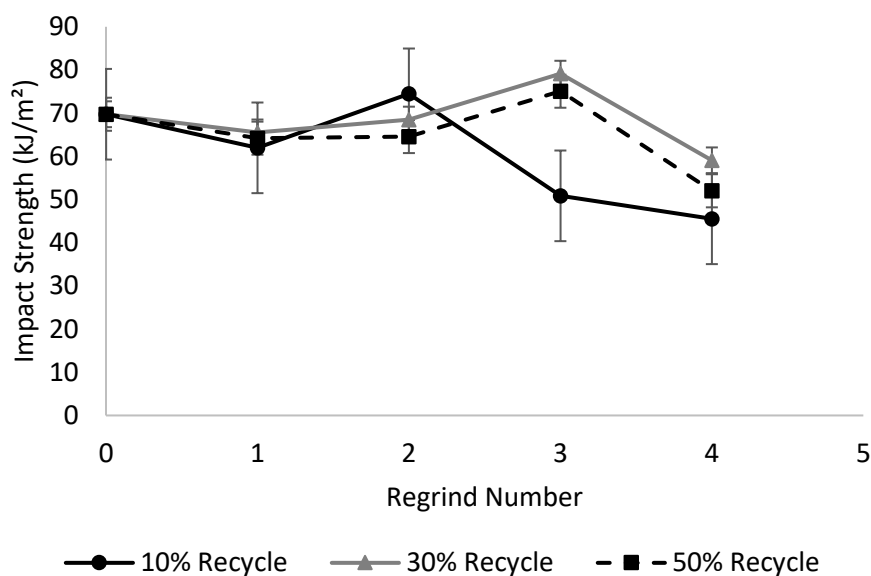


Figure 5.6. Izod impact strength for unnotched specimens taken from Re grind 1-4 LL 8555.25 rotomolded samples with 10, 30 and 50% recycled content

### ***Dart Impact Test***

A dart impact test was performed on Re grind 4 rotomolded samples with the purpose of comparing the results with the Izod impact tester and evaluating a sample's brittleness. Table 5.2 gives the MFE calculated for Re grind 4 samples with 10, 30 and 50% recycled content and the number of brittle failures observed and compares those findings to the virgin sample (Re grind 0). The results shown in Table 5.2 are similar to that of the Izod impact tester where all Re grind 4 samples displayed a lower MFE compared to the virgin sample. Moreover, the Re grind 4 samples

with 30 and 50% recycled content behaved similarly and displayed a higher reported MFE compared to the 10% recycled content sample just as observed in the Izod impact test. Additionally, all Regrind 4 samples displayed brittle failures, likely due to crosslinking restricting chain mobility and flexibility, thus resulting in brittleness. Although the dart impact test was able to validate the apparent decrease in Izod impact strength observed with Regrind 4 samples, a dart impact test was unable to be performed with Regrind 1-3 samples due to limited recycled material available for experiments, thus the overall minimal changes in impact strength for these samples were determined based on conclusions drawn from the Izod test alone.

Table 5.2. MFE for Regrind 4 samples containing 10, 30 and 50% recycled content compared with a virgin LL 8555.25 sample (Regrind 0), along with the number of brittle failures observed

<b>Rotomolded Sample Name</b>	<b>MFE (m.kg)</b>	<b>Number of brittle failures</b>
Regrind 0	9.85	0
Regrind 4, 10%	4.15	2
Regrind 4, 30%	5.7	1
Regrind 4, 50%	5.7	1

#### **5.4.3. Rheology Results**

The complex viscosity is plotted with angular frequency for Regrind 4 samples containing 10, 30 and 50% recycled content and compared with virgin LL 8555.25, shown in Figure 5.7. All samples in Figure 5.7 show similar shear-thinning behaviour. There are small variations in complex viscosity between samples; however, these changes are likely due to experimental noise rather than meaningful variations in material properties. In order to fully interpret these results, the storage ( $G'$ ) and loss modulus ( $G''$ ) were considered.

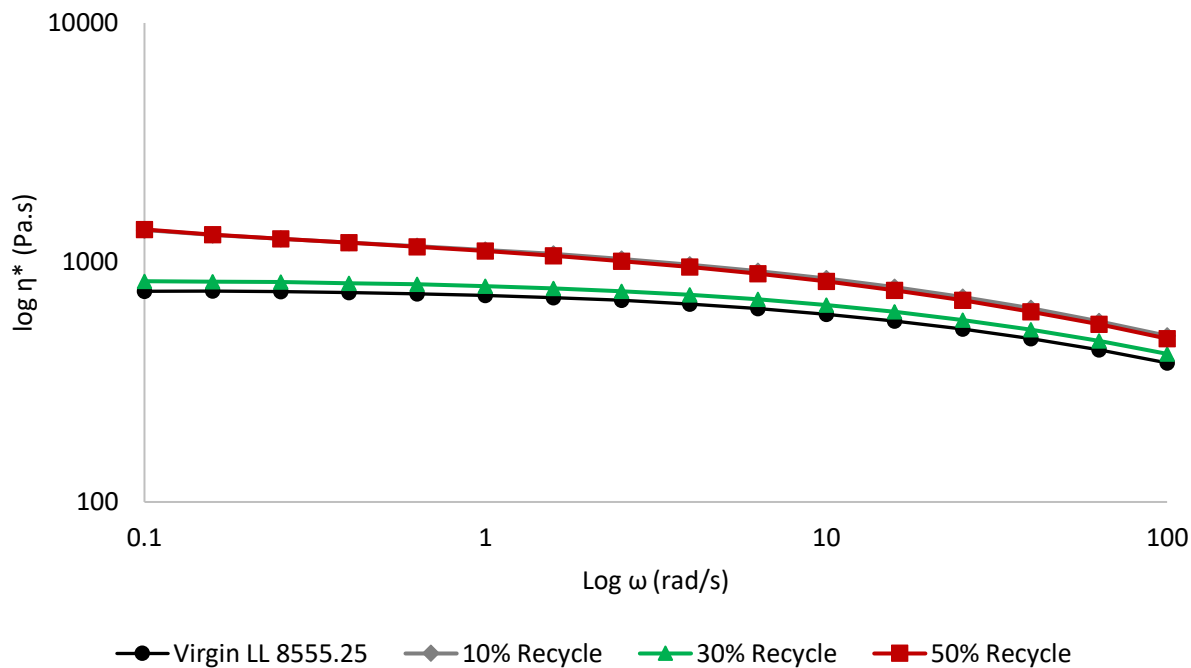


Figure 5.7. Complex viscosity for LL 8555.25 Regrind 4 samples with 10, 30 and 50% recycled content compared to a rotomolded sample with virgin LL 8555.25

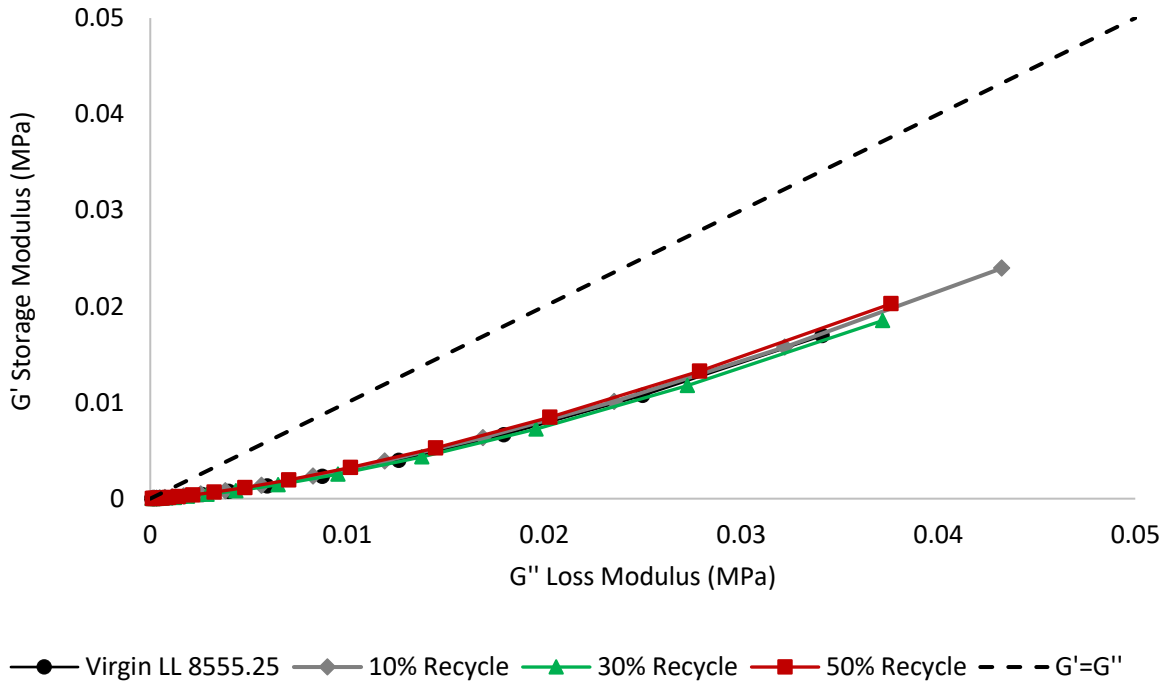


Figure 5.8. Cole-Cole plot for LL 8555.25 Regrind 4 rotomolded samples with 10, 30 and 50% recycled content, compared with a virgin LL 8555.25 rotomolded sample

A Cole-Cole plot for Regrind 4 samples with 10, 30 and 50% recycled content is shown in Figure 5.8 along with a virgin LL 8555.25 rotomolded sample. All of the samples in the figure exhibit almost identical viscoelastic behaviour. The samples are below the  $G' = G''$  line, indicating more viscous behaviour than elastic. The results shown by Figures 5.7 and 5.8 indicate that the samples subjected to the most recycling (Regrind 4) do not show a notable change in polymer microstructure, suggesting that recyclability with LL 8555.25 resin in rotomolding does not significantly impact rheological properties. Although results from Section 5.4.2 show evidence in degradation manifested in a decreased Izod impact strength and increased brittleness for Regrind 4 samples, it is possible that the crosslinking was not severe enough to alter the rheological properties of the samples.

#### **5.4.4. Yellowness Index Results**

The YI of Regrind 1-4 rotomolded samples containing 10, 30 and 50% recycled content is shown in Figure 5.9. The unrecycled virgin LL 8555.25 rotomolded sample displayed a YI of around 23. It is expected that increased recycled content as well as Regrind number would enhance the yellowness of the polymer, thus increasing YI, since thermo-oxidative degradation results in the formation of ketal and aldehyde functionalities that can absorb visible light and give rise to a yellow colour. As seen in Figure 5.9, the samples with 10% recycled content had little to no noticeable colour change. The samples with 30% recycled content showed slight YI increase for all Regrinds compared with to the unrecycled material. For the samples containing 50% recycled content, yellowing significantly increased for Regrinds 2-4. The dramatic increase in YI for samples containing 50% recycled content was attributed to the formation of transformation products from phenolic antioxidants during the course of protecting the polymer from thermo-oxidative degradation rather than from degradation products themselves. This conclusion was

reached because if the yellowing had been exclusively caused by degradation products alone, it would have been accompanied by significant changes in other properties, such as impact strength and viscosity, which was not observed.

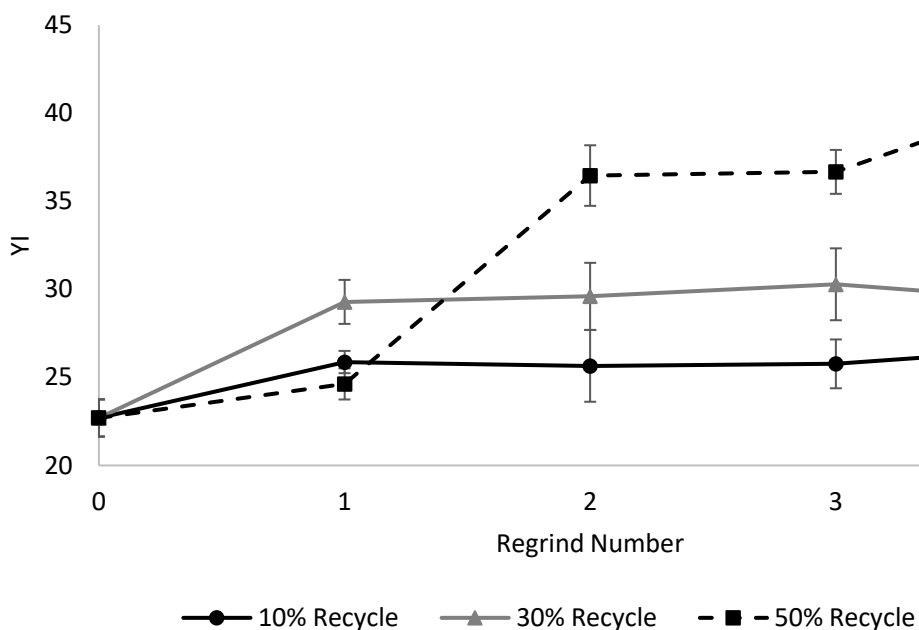


Figure 5.9. Yellowness Index for LL 8555.25 Regrind 1-4 rotomolded samples with 10, 30 and 50% recycled content compared with a virgin LL 8555.25 (Regrind 0) sample

## 5.5. Conclusions

The multi-step granulation recycling with LL 8555.25 provided a more accurate depiction of a PIR recycling process in rotomolding compared to the multi-pass extrusion method presented in Chapter 4. Overall, the LL 8555.25 resin did not show dramatic changes in mechanical or rheological properties compared to the virgin material. A notable decrease in impact strength was only observed for the most heavily recycled material (Regrind 4). It is concluded that the stabilizers in this resin remained effective in alleviating thermo-oxidative degradation effects, at least up until

Regrind 4. The most dramatic change observed in polymer properties was the increase in YI which was most apparent for samples containing 50% recycled content. The increased appearance of yellowing was attributed to the by-products from the phenolic antioxidant generated during the stabilization process, rather than from degradation products themselves since the 50% recycled content samples did not exhibit rheological or mechanical deterioration. These results suggest that recycling PIR in rotational molding is feasible with a sufficiently stabilized resin; however, the extent of recycling must be carefully chosen to avoid excessive discolouration of the final product and potential mechanical losses on heavily recycled material.



## **Chapter 6: Recycling Unstabilized HDPE Resin**

### **6.1. Introduction**

A recycling process involving multi-step granulation of rotomolded samples processed using an unstabilized, reactor grade HDPE 8660 resin will be presented in this chapter. The purpose of recycling an unstabilized resin is to provide a stronger understanding of the degradation effects resulting from recycling without the interference of stabilizers during thermo-oxidative degradation, and to serve as a baseline in studies involving the investigation of the role of different additives which will be presented in the following chapters.

### **6.2. Materials**

The resin used in this recycling process is a completely unstabilized, reactor grade HDPE 8660 powder supplied by Imperial Oil Ltd. This non-commercial resin is referred to as “RG8660” in the studies. The particle size of this resin averaged around 675 microns, which is larger than the typical particle size used in rotomolding (500 microns) since this resin was not commercial pulverized to certain specifications but was instead sampled from the reactor before pelletization, thus a sieving procedure outlined in Section 6.3.1. was performed prior to rotomolding.

### **6.3. Methods**

#### **6.3.1. Sieving Procedure**

The RG8660 powder received from the supplier had a relatively broad particle size distribution with the average size measuring around 675 microns. This is slightly different from rotomolding grades which are normally around 500 microns which facilitates uniform melting and particle sintering during the rotomolding cycle. A particle size distribution comparison between

the RG8660 powder and the stabilized HD 8660.29 powder available commercially is shown in Figure 6.1.

In order to achieve particles sizes suitable for rotomolding, the unstabilized material was sieved. A set of 7 sieves with mesh sizes ranging from 300-2100 microns were stacked on one another above a pan and placed in a RO-TAP sieve shaker. Approximately 150 grams of RG8660 powder was shaken through the stack of sieves for 5 minutes. The powder that was collected from the sieves with mesh sizes less than 500 microns was bagged and used for rotomolding.

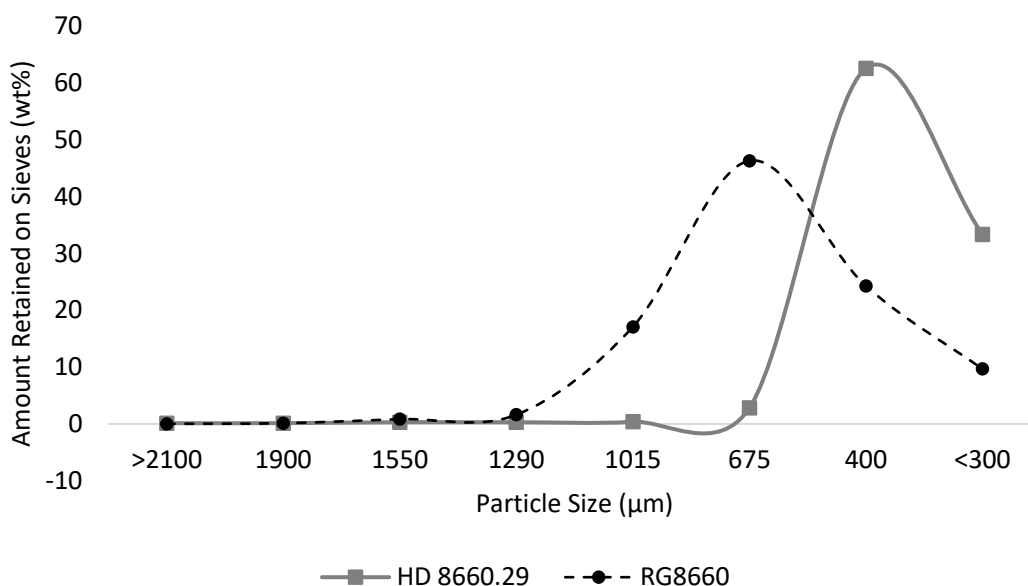


Figure 6.1. Particle size distribution of RG8660 resin compared with HD 8660.29 resin

### 6.3.2. Recycling Process

The resin used for the first rotomolding cycle consisted of sieved RG8660 powdered resin (R0). The recycling process followed the exact procedure as outlined in Section 5.3.1. except a PIAT of 290 °C was used, and only Regrinds 1-3 (R1-3) containing 30% recycled content were tested, to minimize the chances of significant gelation occurring; branching and crosslinking below the gelation point will give better results in terms of modeling trends by mechanical and

rheological testing. A summary of the naming convention for rotomolded RG8660 samples in the study is shown in Table 6.1.

Table 6.1. Rotomolded sample naming convention in multi-step granulation recycling with RG8660

<b>Resin: RG8660</b>	
<i>Rotomolded Sample Name*</i>	<i>No. of times rotomolded RG8660 was ground before reprocessing</i>
<b>R0</b>	0
<b>R1</b>	1
<b>R2</b>	2
<b>R3</b>	3

\*All RG8660 rotomolded samples contained 30 wt% of recycled content except for R0 which contained 0% recycled content

### 6.3.3. Surface Void Analysis

The surface void analysis procedure is the same as outlined in Section 4.3.3.

### 6.3.4. Izod Impact (Unnotched) Test ASTM D4812, ISO 180

The unnotched Izod impact procedure is the same as outlined in Section 5.3.4.

### 6.3.5. Yellowness Index Analysis (ASTM D-1925)

The Yellowness Index Analysis is the same as outlined in Section 5.3.6.

### 6.3.6. Rheological Analysis

The rheological analysis procedure is the same as outlined in Section 5.3.7.

## 6.4. Results and Discussion

### 6.4.1. Rheological Results

The complex viscosity curves for RG8660 rotomolded samples are shown in Figure 6.2. All samples exhibited a shear-thinning behaviour across the entire frequency range. The absence of a clear Newtonian plateau suggests the presence of a more complex microstructure, specifically

the inclusion of crosslinking and LCB which effectively restrict chain mobility and results in a frequency dependent viscosity. At low frequency regions, the complex viscosities between samples varied significantly where large-scale molecular motion is more prevalent, suggesting that the rotomolded samples are composed of different molecular structures in a relaxed state. The samples tested were obtained directly from a rotomolded box, meaning that the polymer had already gone through the thermo-oxidative degradation effects during the rotomolding cycle. Thus, the increase in complex viscosity as the Re grind number increases indicates a progressive increase in the degree of crosslinking and LCB due to thermo-oxidative degradation in the rotomolding unit. As angular frequency increased, the complex viscosities converged for all samples suggesting that the materials' molecular chains responded similarly at higher deformation rates and more importantly, the shear thinning nature of PE was becoming greater. To further interpret the viscoelastic properties of the samples, a Cole-Cole plot is shown in Figure 6.3.

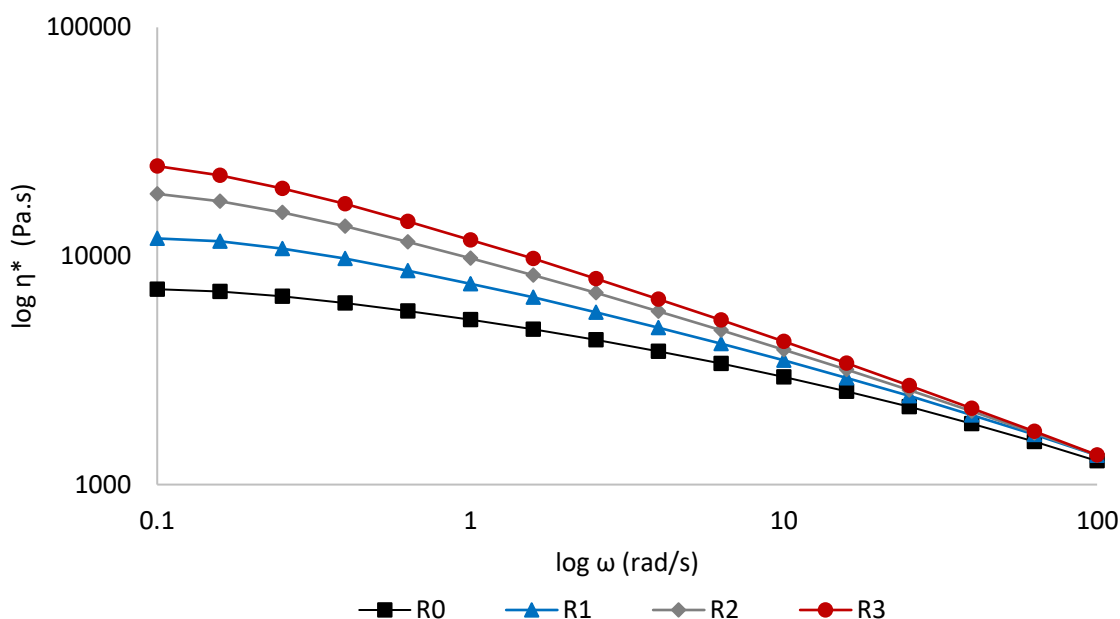


Figure 6.2. Complex viscosity with increasing angular frequency for RG8660 Re grind 1-3 samples compared with virgin RG8660

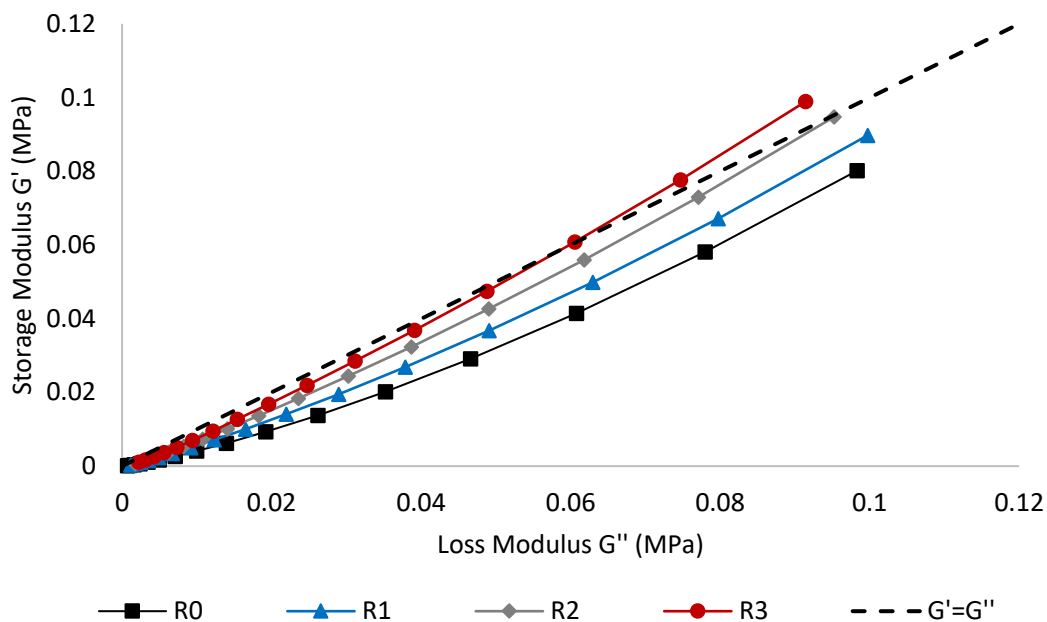


Figure 6.3. Cole-Cole plot for RG8660 Regrind 1-3 samples compared with a virgin RG8660 sample (Regrind 0)

The Cole-Cole curve for R0 is completely below the  $G'=G''$  line, indicating a dominant viscous behaviour of the material. As the Regrind number increased, the Cole-Cole curves shifted closer to the  $G'=G''$  line, and by R3 the curve began to swing into the elastic dominant region. This shift towards the elastic region as Regrind number increased is attributed to restricted chain mobility and increased stiffness due to crosslinking which ultimately enhances the material's ability to store elastic energy. R3 was the first condition where crosslinking and branching occurred to sufficient degree that the changes in molecular structure were detectable though some degradation was likely to also be occurring in the earlier recycling steps to an undetectable extent. It was somewhat surprising that the polyethylene, without stabilizer, showed so little microstructural changes until R3 considering the long heating history.

### 6.4.2. Results of Surface Void Analysis

A surface void analysis was performed on R1-3 rotomolded samples and compared with a virgin RG8660 sample (R0), shown in Figure 6.4. The total surface void area for R0 was approximately 7%, significantly exceeding the typical desirable amount in rotomolding, which should be less than 1%. As the Regrind number increased, the percentage of surface void area generally increased as well, indicating steadily poorer sintering behaviour with repeated recycling. This behaviour is attributed to the increasing zero-shear viscosity resulting from thermo-oxidative degradation, yielding slower melt bridging and less melt coalescence before PIAT was reached. The increase in viscosity is validated by the rheological analysis of rotomolded samples in the previous section.

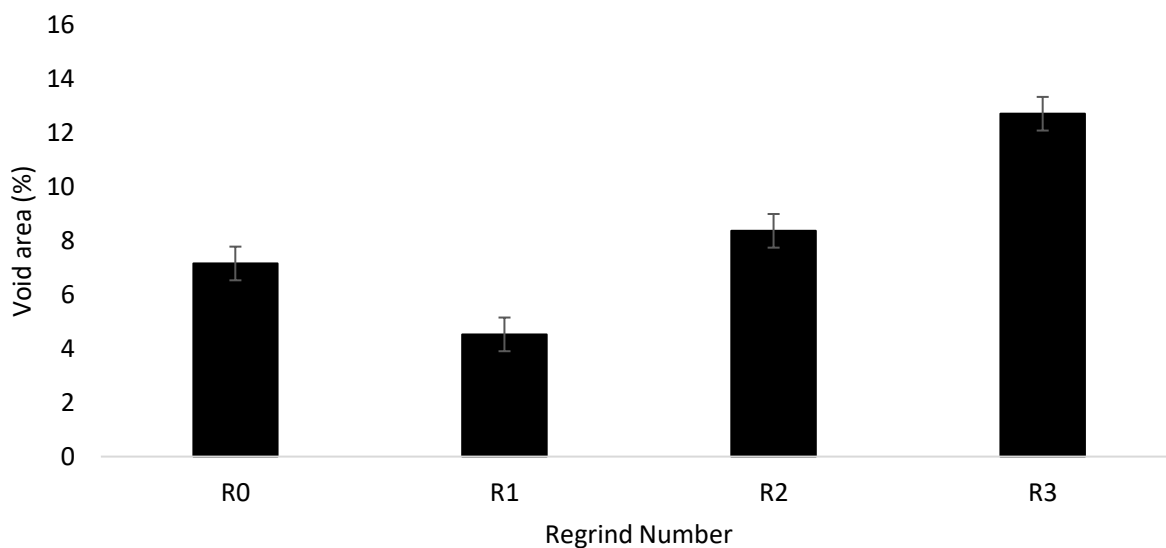


Figure 6.4. Surface void area of RG8660 Regrind 1-3 rotomolded samples compared with virgin RG8660 (R0)

### 6.4.3. Izod Impact Strength Results

The Izod impact strength is reported for unnotched specimens taken from R1-3 samples and compared with the virgin RG8660 sample (R0), shown in Figure 6.5. The impact strength for R0 was approximately 55 kJ/m<sup>2</sup> and as the Regrind number increased, the impact strength decreased, with a most dramatic drop observed for Regrind 3. The large standard deviations between specimens may be due to the air bubbles trapped in the polymer caused by incomplete sintering, which created significant weak points in the sample. Depending on where the Izod impact hammer hits a specimen, this can cause large deviations in impact strength testing for a given sample.

Table 6.2 shows the percent of specimens which displayed ductile versus brittle fractures upon impact for all of the RG8660 samples. As recycling increased, the number of brittle failures increased due to increased crosslinking which generated an overly rigid (elastic) polymer structure, unable to deform before failure; the trend matches that seen in the Cole-Cole plot.

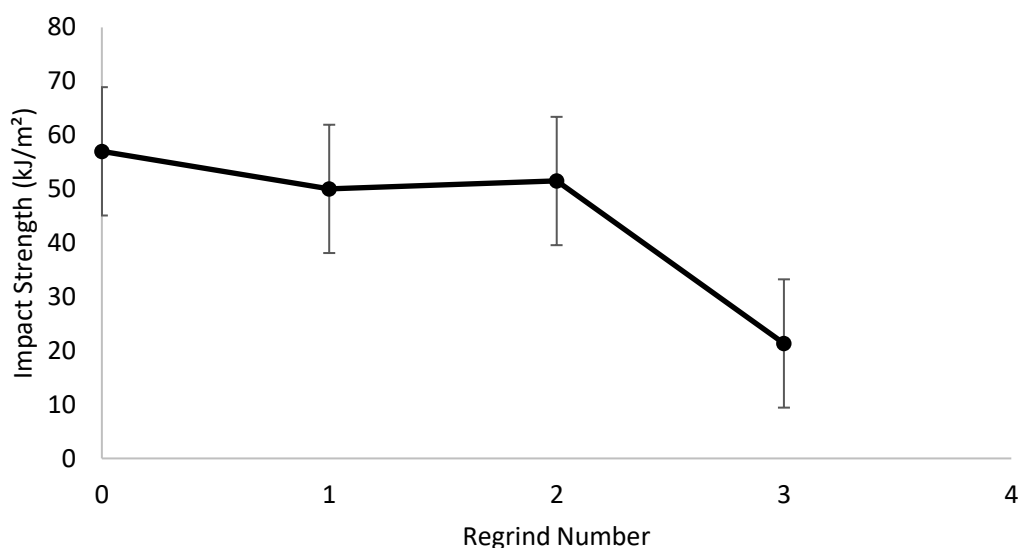


Figure 6.5. Izod impact strength for RG8660 Regrind 1-3 rotomolded samples with 30% recycled content compared to virgin RG8660 (R0)

Table 6.2. Percentage of ductile and brittle fractures observed during unnotched Izod testing for RG8660 rotomolded samples

<b>Rotomolded sample name</b>	<b>% Ductile Fractures</b>	<b>% Brittle Fractures</b>
<b>R0</b>	80	20
<b>R1</b>	80	20
<b>R2</b>	60	40
<b>R3</b>	20	80

#### **6.4.4. Yellowness Index Results**

The YI of R1-3 rotomolded samples was compared with the virgin RG8660 rotomolded sample (R0), shown in Figure 6.6. The YI for R0-2 samples remained steady around a value of 23, until R3 where the YI is increased to approximately 25. Despite significant deterioration observed with mechanical and rheological properties of the recycled RG8660 material, only a slight increase in YI was detected with recycling. This will be an important point of consideration for the next chapter since it indicates that thermo-oxidative degradation, in the absence of stabilizers, makes minimal contributions to the appearance of yellowness in rotomolded products.



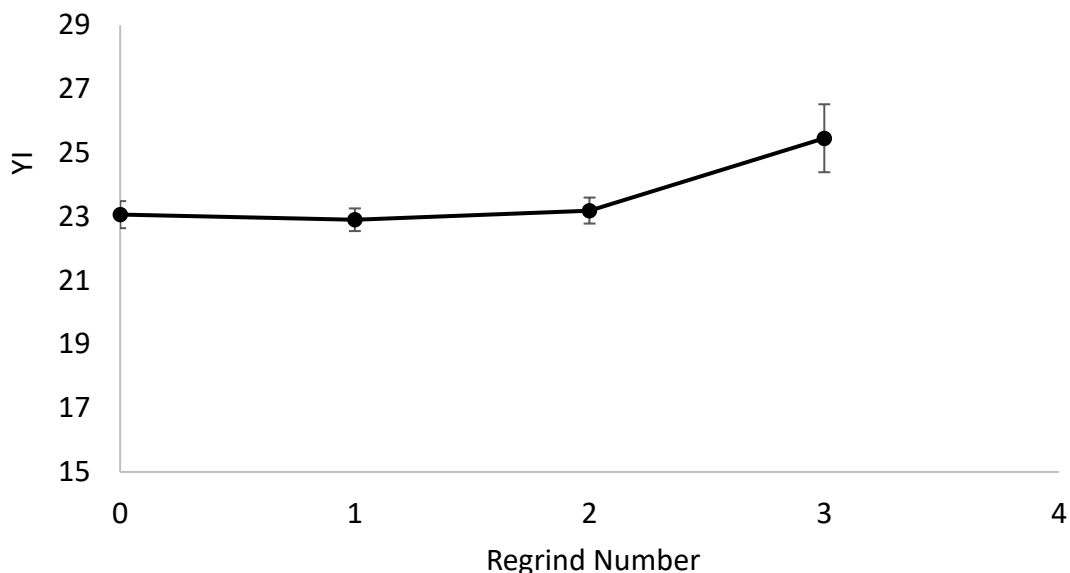


Figure 6.6. Yellowness Index for RG8660 Regrind 1-3 rotomolded samples compared with a rotomolded virgin RG8660 sample (R0)

## 6.5. Conclusions

The multi-step granulation recycling process with unstabilized RG8660 resin revealed substantial changes in polymer properties, confirming the potential for thermo-oxidative degradation with recycled polyethylene during rotomolding. Rheological analysis detected changes in polymer microstructure signifying an increase in crosslinks and branches in the recycled resin, which was observed to produce poor sinter-ability, deteriorated impact strength and increased brittleness. Despite these obvious signs of degradation, only a minimal change in YI was observed, signifying that the carbonyl groups generated by thermo-oxidative degradation did not have a significant role in polymer discolouration during recycling.

These observations provided a clearer understanding of the consequences associated with thermo-oxidative degradation in the absence of stabilization additives during repeated processing of the polymer in the rotomolder.

## **Chapter 7: Recycling with HDPE Blends**

### **7.1. Introduction**

This chapter explores recycling involving the multi-step granulation method using a blend of stabilized and unstabilized HDPE resins. The purpose of recycling with this blend is to investigate whether the pre-stabilized commercial HDPE resin can act as an additive to mitigate degradation effects. This investigation is intended to provide industries with a strategy to alleviate degradation effects experienced with less stabilized resins by blending with small quantities of a more highly-stabilized commercial resin on hand. Physical, mechanical and rheological properties of these recycled blends will be compared with results from Chapter 6.

### **7.2. Materials**

The resins used in this chapter consist of the same reactor grade HDPE 8660 resin (RG8660) studied in Chapter 6, along with the same stabilized high-density polyethylene commercial resin studied in Chapter 4, (ExxonMobil™ HD 8660.29), which contains a proprietary mixture of both antioxidants and UV stabilizers. Both resins were supplied by Imperial Oil Ltd. The blended samples will be referred to as “HD Blend”.

### **7.3. Methods**

#### **7.3.1. Recycling Procedure**

The polymer powder used for the first rotomolding cycle was a blend consisting of 30 wt% of HD 8660.29 and 70 wt% of sieved RG8660 powdered resin. This sample was referred to as “HD Blend”. The recycling process was exactly as outlined in Section 6.3.2. except with each Regrind, the ground HD Blend sample was blended with 70 wt% of virgin RG8660 resin. Thus, with each successive regrind, the concentration of the stabilized resin diminished. The recycling

process was only completed with Re grind 1 and 2 samples containing 30% recycled content. A summary of the naming convention for HD Blend rotomolded samples is shown in Table 7.1.

Table 7.1. Summary of the naming convention for HD Blend rotomolded samples

<i>Rotomolded Sample Name</i>	<i>Resin blend 30/70 (wt%)</i>	<i>Number of times rotomolded HD Blend was ground before reprocessing</i>
<b>HD Blend</b>	HD 8660.29/RG8660	0
<b>HD Blend R1</b>	HD Blend/RG8660	1
<b>HD Blend R2</b>	HD Blend/RG8660	2

### 7.3.2. Surface Void Analysis

A surface void analysis was performed the same way as described in Section 4.3.3.

### 7.3.3. Izod Impact (Unnotched) Test ASTM D4812, ISO 180

The unnotched Izod impact procedure is the same as outlined in Section 5.3.4.

### 7.3.4. Yellowness Index (ASTM D-1925)

The Yellowness Index Analysis is the same as outlined in Section 5.3.6.

### 7.3.5. Rheological Analysis

The rheological analysis procedure is the same as outlined in Section 5.3.7.

## 7.4. Results and Discussion

### 7.4.1. Rheological Results

The complex viscosities for HD Blend R2 along with RG8660 R2 samples are compared in Figure 7.1 for the purposes of investigating whether the stabilizers left in the most recycled HD Blend sample (R2) remained sufficient in alleviating degradation effects experienced by the

unstabilized material subject to the same amount of recycling (RG8660 R2). A comparable shear thinning behaviour for both samples is observed in Figure 7.1, except the HD Blend displays a significantly lower viscosity throughout the entire frequency range, likely due to a decrease in the degree of crosslinks.

The viscoelastic behaviours of the samples were further investigated via a Cole-Cole plot, shown in Figure 7.2. The curves are overlapping suggesting that both samples exhibited a similar balance between how energy is stored and dissipated; however, the HD Blend curve is considerably lesser in magnitude compared to the RG8660 sample. This indicates that the RG8660 blend had an overall larger storage and loss modulus, reflecting greater stiffness which is also attributed to a greater degree of crosslinking, corresponding to the larger viscosity shown in Figure 7.1. Thus, it can be concluded that the stabilizers in the HD Blend interfered with the degradation experienced by the RG8660 sample during recycling.

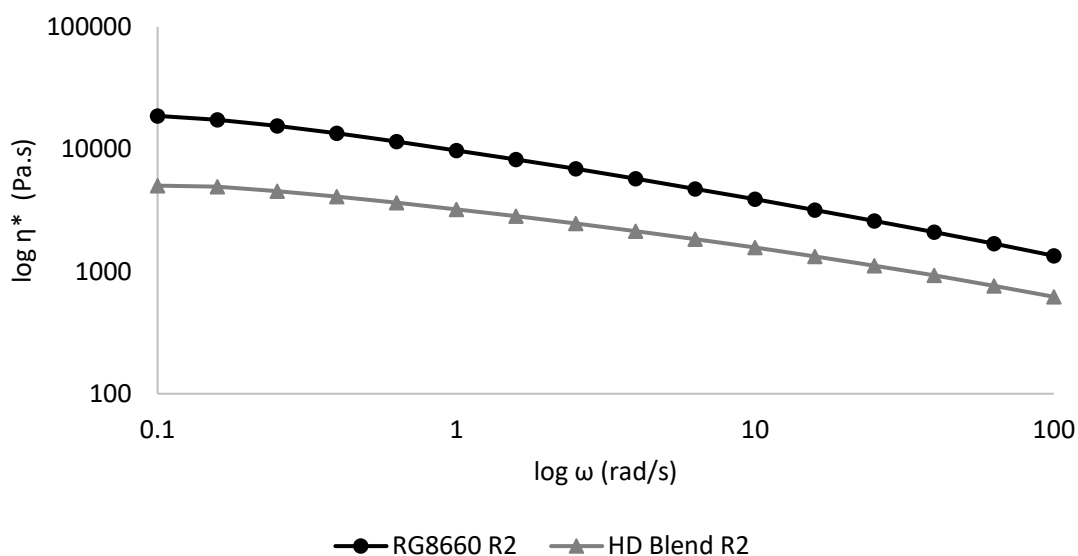


Figure 7.1. Complex viscosity of a rotomolded RG8660 R2 sample compared to an HD Blend R2 sample

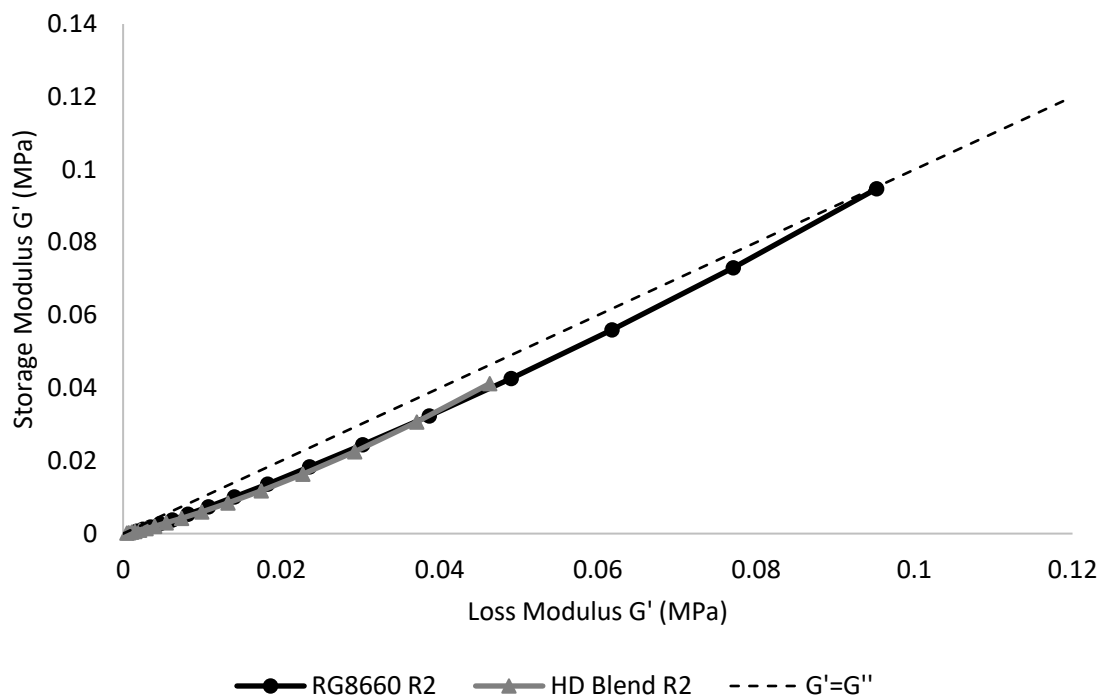


Figure 7.2. Cole-Cole plot for a rotomolded RG8660 R2 sample compared with an HD Blend R2 sample

#### 7.4.2. Surface Void Analysis Results

A surface void analysis was conducted on HD Blend R0-2 rotomolded samples and compared with results obtained from the RG8660 R0-2 samples, shown in Figure 7.3. The void area on the surface of all samples was relatively large, exceeding 4%, which is substantially greater than the desired <1% void area for rotomolding, indicating an overall poor sinter-ability for all samples. However, the void area on the HD Blend samples was generally less compared to the RG8660 samples, with the most notable decrease for R2. The stabilizers present in the HD Blends are responsible for decreasing the viscosity of the polymer melts, which was validated through rheological analysis, thus promoting greater particle sintering ability.

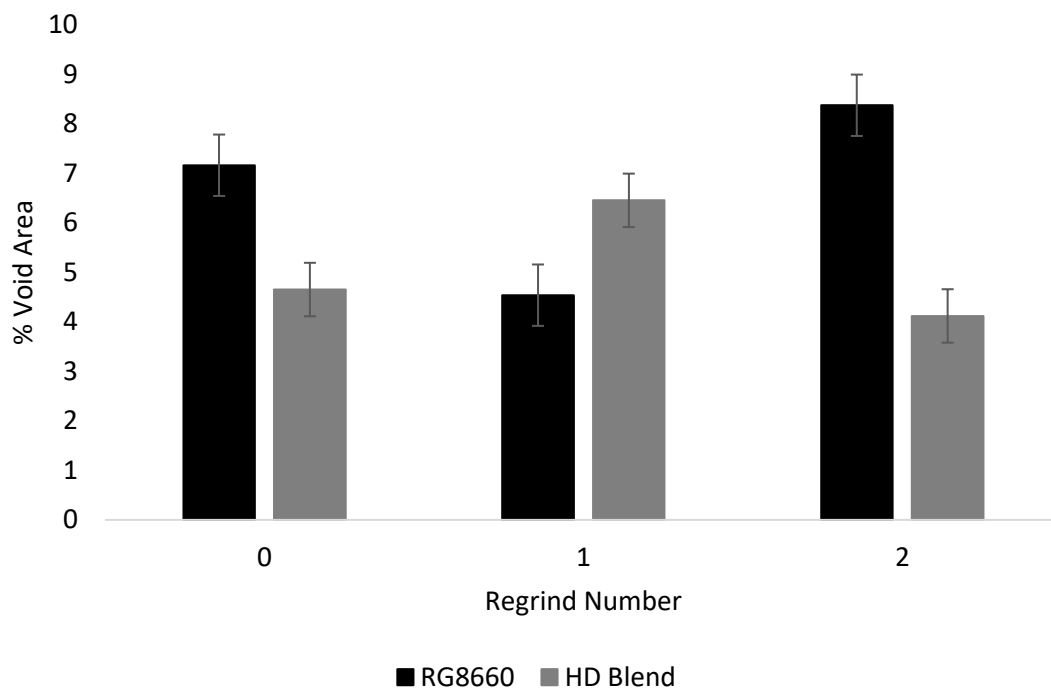


Figure 7.3. Surface void analysis for Regrind 0-2 samples made with HD Blend compared with RG8660

#### 7.4.3. Izod Impact Strength Results

Izod impact strength was reported for HD Blend R0-2 samples and compared with RG8660 R0-2 samples, shown in Figure 7.4. Compared to the HD 8660.29 resin studied in Chapter 4, the magnitude of Izod impact strength observed with the HD Blends is significantly higher, averaging around  $55 \text{ kJ/m}^3$ , whereas the average Izod strength observed in Chapter 4 was approximately  $17 \text{ kJ/m}^3$ . This large discrepancy in impact strength is attributed to the fact that the specimens examined in Chapter 4 were notched whereas the specimens in this Chapter were unnotched. The notch during impact testing acts as a stress concentrator allowing for a crack to propagate more easily, thus resulting in a significantly lower impact strength compared to unnotched specimens. There is a general decrease in impact strength as the regrind number increases for the HD Blend

samples, shown in Figure 7.4, which may be due to the diminishing concentration of stabilizers with each successive regrind, and thus there is a decreasing amount protection from thermo-oxidative degradation effects. When comparing the impact strength between HD Blends and RG8660 samples, it appears that the HD Blends had a higher impact strength for Regrinds 0 and 1, although the size of the error bars indicate that this increase is not statistically meaningful. The large standard deviations between specimens may be attributed to incomplete sintering, as detected by the surface void analysis, creating air pockets within the rotomolded sample which can cause significant weak points and large deviations in impact strength depending on where the Izod impact hammer strikes the specimen. It is possible that using a higher concentration of stabilized resin would offer more dramatic and statistically significant changes in impact strength.

Tables 7.2 and 7.3 compare the percentage of specimens between the HD Blends and RG8660 samples which exhibited ductile and brittle failure, respectively. The HD Blend displayed an overall lower number of ductile failures compared to the RG8660 samples and did not show any signs of brittle fracture. The absence of brittle fracture in the HD Blends indicates a level of success in alleviating excessive crosslinking which would otherwise result in an overly brittle structure as demonstrated by the RG8660 samples.

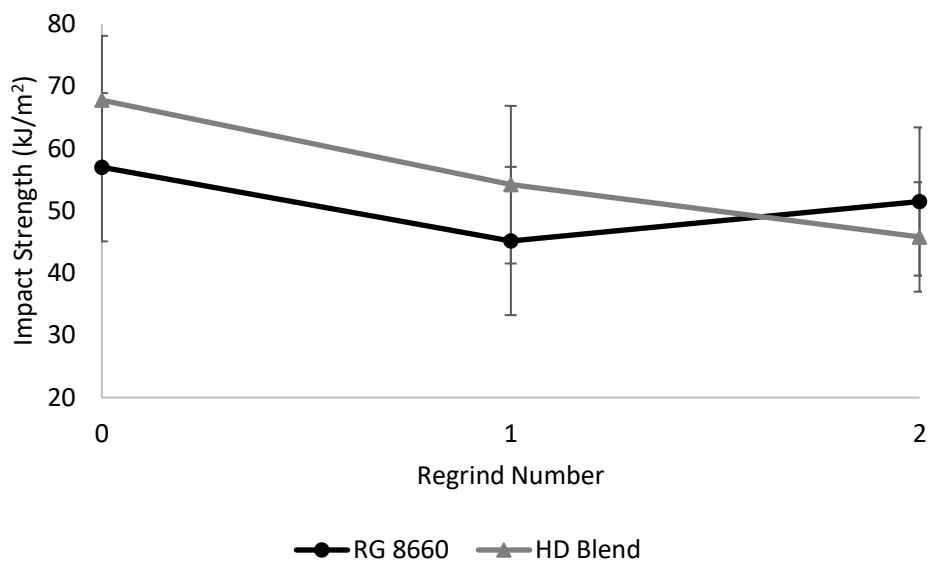


Figure 7.4. Izod impact strength for Regrind 0-2 samples processed using a 30/70 blend of HD 8660 resin and unstabilized RG8660 resin, and compared with samples processed with unstabilized resin (RG8660)

Table 7.2. Percentage of ductile fractures observed during unnotched Izod testing for all HD Blend samples compared with RG8660 rotomolded samples

% Ductile Failures		
Sample Name	<i>RG8660</i>	<i>HD Blend</i>
<b>R0</b>	80	60
<b>R1</b>	80	60
<b>R2</b>	60	80

Table 7.3. Percentage of brittle fractures observed during unnotched Izod testing for all HD Blend samples compared with RG8660 rotomolded samples

% Brittle Failures		
Sample Name	<i>RG8660</i>	<i>HD Blend</i>
<b>R0</b>	20	0
<b>R1</b>	20	0
<b>R2</b>	40	0



#### 7.4.4. Yellowness Index Results

The YI was reported for all HD Blend samples and compared with RG8660 samples, shown in Figure 7.5. As the regrind number increases, there is a steady increase in YI for HD Blend samples compared to a near-constant YI value observed for RG8660 samples. Additionally, the YI for the HD Blend samples is lower than the RG8660 samples until R2 where it surpasses the YI for the RG8660 sample. Since rheological and surface void analysis confirmed the effectiveness of stabilizers alleviating crosslinking effects observed in R2 samples, it is speculated once again that the increased yellow appearance for HD Blend R2 is mainly attributed to the intermediate products formed by the stabilizers during the course of protecting the polymer, whereas the yellowing shown by the RG8660 samples is solely from the formation of oxidation products.

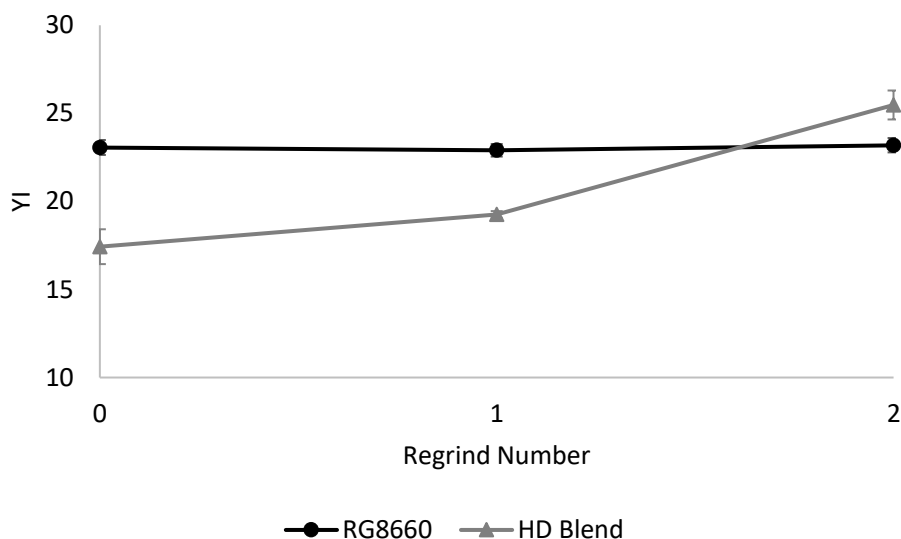


Figure 7.5. YI for all HD Blends compared with RG8660 samples

## 7.5. Conclusions

The results obtained in this section highlight the significant impact that a small amount of pre-stabilized commercial resin can provide in mitigating thermo-oxidative degradation effects experienced by an unstabilized resin during the course of recycling. Even with diminishing amounts of stabilizers with repeated recycling, the most heavily recycled samples (R2) continued to demonstrate the stabilizers' ability in reducing excessive crosslinking, as revealed through rheological and sintering analyses. Although no clear distinctions were observed in the magnitude of impact strength between the HD Blend and RG8660 samples, samples containing stabilizers did not exhibit any brittle fractures, indicating a reduction in the degree of crosslinking. These results suggest that blending a pre-stabilized resin with a degraded polymer can prove to be beneficial, although in order to achieve more significant improvements in mechanical performance, increasing the concentration of stabilized resin should be considered. Since the stabilizers present in the HD 8660.29 resin are known to be a combination of antioxidants and UV stabilizers, it remains unclear whether one additive is responsible for alleviating degradation effects or if the combination of both reveals synergistic properties. Thus, the following chapter will explore a recycling process in which an antioxidant and a UV stabilizer are each separately blended with an unstabilized resin to gain a better understanding of the roles that each additive plays during recycling.

## **Chapter 8: Additives in Recycling**

### **8.1. Introduction**

A multi-step granulation recycling procedure with rotomolded samples consisting of an unstabilized HDPE resin individually compounded with an antioxidant, a UV stabilizer and a blend of both will be investigated in this chapter. The goal is to compare each compounded sample with one another as well as with the unstabilized samples studied in Chapter 6 (RG8660) to gain a deeper understanding of the purpose that individual additives serve during recycling. Results of physical, mechanical and rheological properties will be examined.

### **8.2. Materials**

The unstabilized resin used for this study was identical to the resin studied in Chapter 6 (RG8660). The first additive explored was a UV stabilizer with a trade name of “Cyasorb Cynergy Solutions® M528 Light Stabilizer” supplied by Cytec Canada Inc. This stabilizer was referred to as “Cyasorb”. The second additive examined was an antioxidant with a trade name of “Cyanox® 2777 Antioxidant” supplied by Cytec Canada Inc. and it was referred to as “Cyanox” in this study.

### **8.3. Methods**

#### **8.3.1. Additive Compounding Method**

A total of three formulations were prepared by melt compounding prior to the recycling trials. Formulations 1-3 consisted of 0.1 wt% of Cyanox with RG8660, 0.1 wt% of Cyasorb with RG8660 and finally 0.05 wt% of both Cyasorb and Cyanox with RG8660, respectively. The components of Formulations 1-3 along with their respective weight percentages are summarized in Columns 1-4 on Table 8.1. A total of 500 grams of powder for each formulation was prepared by manually dry blending all of the respective components in a polyethylene bag and then tumbling

the bag for 10 minutes to achieve homogeneity prior to melt compounding. An 18 mm Leistritz MICRO18 Co-Rotating Twin Screw Extruder was used to process each formulation. A fixed barrel temperature profile was used, ranging from 160-180 °C along its barrel zones, and the screw design used is shown in Appendix A. The extruder screw was designed with the intention to incorporate sufficient kneading blocks to ensure effective and uniform dispersion of the additives, while also striving to minimize shear stresses that can degrade the polymer in the extruder. The extruded material for each formulation was pelletized and bagged prior to recycling. The sample names of the extruded formulations are summarized in Column 5 of Table 8.1.

Table 8.1. Components of formulations 1-3 along with their respective weight percentages and extruded formulation sample names

<i>Formulation No.</i>	<i>RG8660 (wt%)</i>	<i>Cyanox (wt%)</i>	<i>Cyasorb (wt%)</i>	<i>Extruded Sample Name</i>
<b>1</b>	99.9	0.1	0	ANT
<b>2</b>	99.9	0	0.1	UV
<b>3</b>	99.9	0.5	0.5	ANTUV

### 8.3.2. Recycling Procedure

The recycling procedure for all formulations was conducted in the same manner. First, 30 grams of the extruded formulation pellets (~3 mm dia.) were reduced in size via a grinding mill (Kinematica Polymix PX-MFC 90D, Switzerland) with a 0.5 mm sieve and then manually blended with 70 grams of RG8660. Next, the rotomolding cycle was conducted as outlined in Section 3.1 with a PIAT of 215°C and an oven temperature of 290°C. Two faces of a rotomolded box were set aside for characterization while the remaining faces were first fed into a plastic granulator followed by the same grinding mill with a 0.5 mm sieve. A mixture of 30 g of ground powder and 70 g of

fresh RG8660 powdered resin was manually blended before charging the mold and repeating the rotational molding process. This entire procedure was repeated to obtain a total of 3 recycled regrind conditions for each formulation. A summary of the naming convention for all of the stabilized rotomolded samples in this section is outlined in Table 8.2.

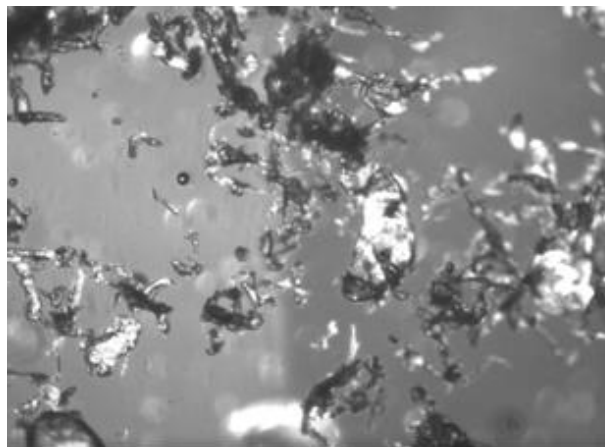
Table 8.2. Summary of stabilized rotomolded sample naming convention

<i>Stabilized Rotomolded Sample Name</i>	<i>Resin blend 30/70 (wt%)</i>	<i>Number of times rotomolded sample was ground before reprocessing</i>
<b>ANT R0</b>	ANT/RG8660	0
<b>ANT R1</b>	ANT R0/RG8660	1
<b>ANT R2</b>	ANT R1/RG8660	2
<b>UV R0</b>	UV/RG8660	0
<b>UV R1</b>	UV R0/RG8660	1
<b>UV R2</b>	UV R1/RG8660	2
<b>ANTUV R0</b>	ANTUV/RG8660	0
<b>ANTUV R1</b>	ANTUV R0/RG8660	1
<b>ANTUV R2</b>	ANTUV R1/RG8660	2

No rotomolded samples were possible with the original extruded materials to give baseline properties since the highly irregular particle shapes and sizes produced in the grind mill showed poor sinter-ability without the RG8660 present; the grinding process involves mechanical forces such as compression and shear with simultaneous heat generation which may lead to particle agglomeration and irregular particle shapes. A microscope at 6x magnification was used to capture images of the particles obtained from grinding the extruded sample “ANT” via a grinding mill

with a 0.5 mm sieve size and compared them with the particles of the virgin RG8660 powdered resin obtained from the supplier, shown in Figures 8.1 (A) and (B) respectively. The particles of the RG8660 resin shown by Figure 8.1 (B) exhibit a consistent size distribution with minimal variations in shape whereas the particles resulting from the grinding mill in Figure 8.1 (A) exhibit a non-uniform, flake-like morphology with numerous protruding extensions. A highly irregular particle distribution results in poor sintering of the particles during melting due to poor particle packing, causing excessive trapped air pockets which are unable to diffuse during melting. Thus, when a sample consisting of 100% powder obtained via the grinding mill was rotomolded, the resulting box exhibited highly uneven wall thicknesses which prevented characterizations to be completed. Figures 8.2 (A) and (B) compare rotomolded samples processed using 100% powder obtained via the grinding mill with a 0.5 mm sieve of extruded sample “ANT”, versus a blend consisting of 70 wt% of virgin RG8660 and 30 wt% of ground “ANT” powder obtained via the grinding mill, respectively. As shown by Figure 8.2 (A), the sample processed using 100% ground material displays significant wall irregularities, specifically around the edges of the box and a more pronounced yellow colour, likely due to the higher concentration of stabilizers present in the sample. In comparison, when blended with 70 wt% of virgin RG8660 shown in Figure 8.2 (B), the uniformity of the RG8660 particles provided sufficient packing of the particles in the bulk, resulting in a more uniform final product. Thus, the blending of the extruded samples with RG8660 was required in order to properly carry out characterizations on the part; however, doing this significantly diminished the concentration of stabilizers in the blend. Specifically, after blending 70 wt% of RG8660 with 30 wt% of an extruded sample, the stabilizer concentration reduced from 0.1 wt% to 0.03 wt%. This concentration was further diminished as the recycling process was carried out.

(A)



(B)

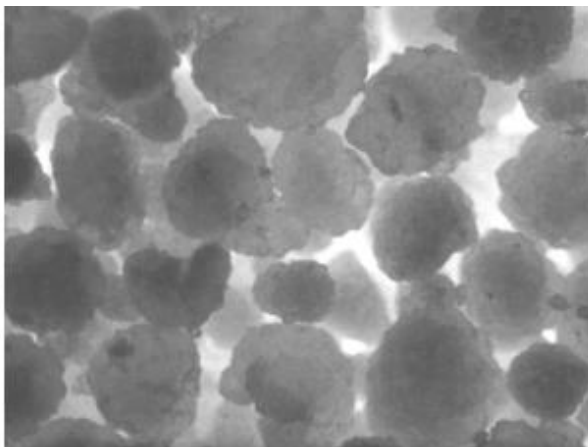


Figure 8.1. Microscopic images with a 6x magnification level of (A): powder obtained via the grinding mill with a 0.5 mm sieve of extruded sample “ANT” and (B): RG8660 powdered resin obtained from supplier

(A)



(B)



Figure 8.2. Photo of a rotomolded box processed using: (A) 100% powder obtained via the grinding mill with a 0.5 mm sieve of extruded sample “ANT” and (B) a blend of 70 wt% virgin RG8660 powder and 30 wt% of ground “ANT” powder obtained from the grinding mill

### **8.3.3. Rheological Analysis**

The rheological analysis procedure is the same as outlined in Section 5.3.7.

### **8.3.4. Surface Void Analysis**

A surface void analysis was performed the same way as described in Section 4.3.3.

### **8.3.5. Izod Impact (Unnotched) Test ASTM D4812, ISO 180**

The unnotched Izod impact procedure is the same as outlined in Section 5.3.4.

### **8.3.6. Yellowness Index (ASTM D-1925)**

The Yellowness Index Analysis is the same as outlined in Section 5.3.6

## **8.4. Results and Discussion**

### **8.4.1. Rheological Results**

The complex viscosities of the stabilized rotomolded samples subject to the most recycling (R2) were compared with RG8660 R2 in order to investigate how each type of stabilizer contributed to the recycled part properties by comparison to those made with the unstabilized material and subject to the same amount of recycling. The results are shown in Figure 8.3. All samples displayed an almost identical shear thinning behaviour, except the RG8660 sample exhibited a slightly higher complex viscosity; the result with RG8660 confirmed the test conditions should produce degradation when stabilizers are not present. It is possible that each stabilized sample contributed equally to reducing the crosslink density of the unstabilized material; however, the percent difference of complex viscosities between the stabilized samples and the RG8660 sample was approximately 20% across the entire frequency range which is relatively small and may be due to experimental noise rather than representing meaningful transformations in material



properties. To further analyze the rheological characteristics of the samples, a Cole-Cole plot is shown in Figure 8.4.

All of the curves on the Cole-Cole plot displayed a similar balance between storage and loss modulus indicated by their close alignment to one another in Figure 8.4. However, the RG8660 curve was slightly longer in moduli magnitude compared to the stabilized samples suggesting an overall greater stiffness which may be attributed to a higher degree of crosslinking linked to the exclusion of additives. Similar to the complex viscosities, this change in viscoelastic behaviour was minimal which may simply be due to experimental variability rather than significant changes in microstructure. To further interpret these results, it was necessary to examine performance characteristics of the samples.

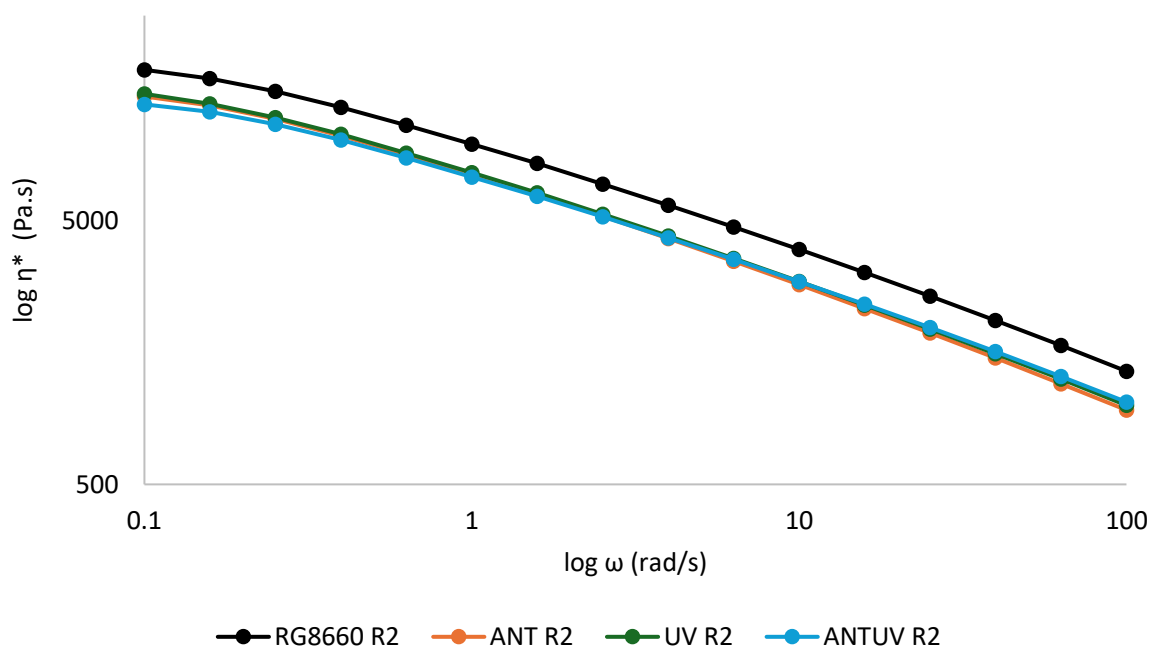


Figure 8.3. Complex viscosities for all stabilized rotomolded samples subject to Re grind 2 (R2) compared with a RG8660 R2 sample

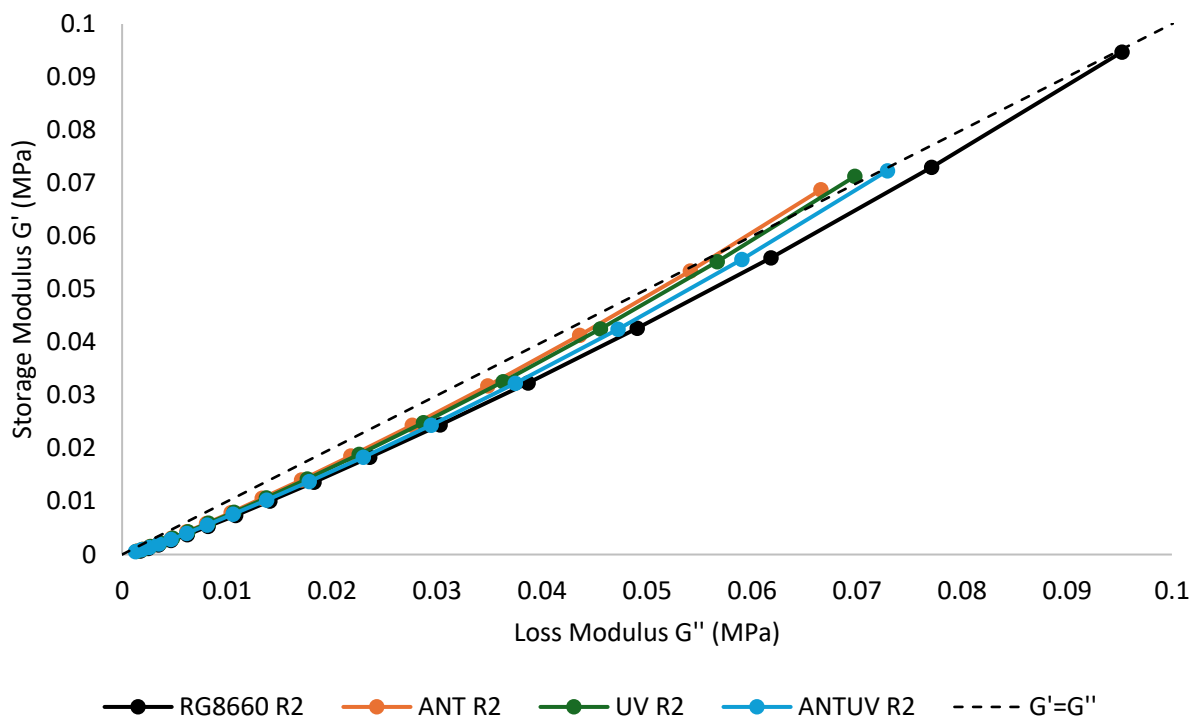


Figure 8.4. Cole-Cole plot for all stabilized rotomolded samples subject to Re grind 2 (R2) compared with a RG8660 R2 sample

#### 8.4.2. Surface Void Analysis Results

A surface void analysis was conducted on all stabilized rotomolded samples and compared with results obtained from the RG8660 samples, shown in Figure 8.5. The void area on the surface of all samples was relatively large, exceeding 4%, which is significantly greater than the desired <1% void area for rotomolding, suggesting overall poor sintering for all samples. In general, the “ANTUV” sample containing both antioxidant and UV additives displayed a lower void area compared to the other samples, which was especially evident for the R2 samples, indicating possible synergetic effects in sinter-ability when combining stabilizers. It remains unclear whether the antioxidant or UV additives provided better sintering on their own compared to the unstabilized samples during recycling.

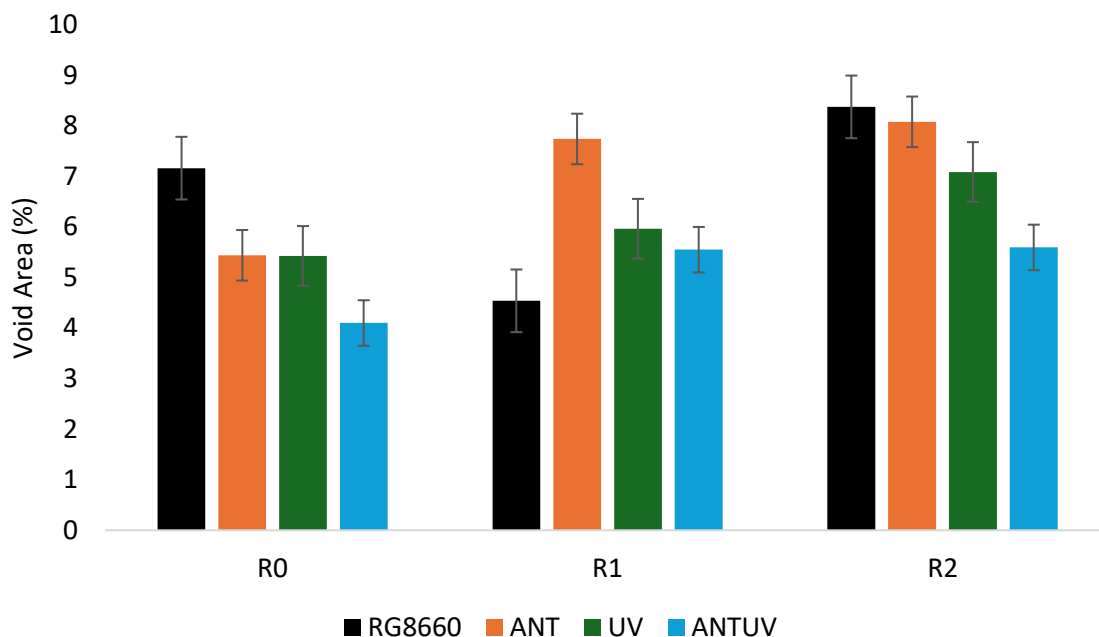


Figure 8.5. Surface void analysis for all stabilized rotomolded samples compared with RG8660 samples

#### 8.4.3. Izod Impact Results

Izod impact strength was reported for all of the stabilized rotomolded samples and compared with RG8660 samples, shown in Figure 8.6. Considering the variability between specimens for each sample, there was only a distinct increase in impact strength for the ANTUV R2 sample, containing both UV and antioxidant additives. This may indicate a potential synergy between the additives, allowing them to work together to more effectively alleviate mechanical degradation effects which is a similar observation found through sintering analysis. However, given the small variations between samples and large standard deviations between specimens, it is difficult to say with confidence that the apparent increase in impact strength observed with sample ANTUV R2 was statistically significant or if it was merely an anomaly. Further testing with a

greater number of replicates is required for confirmation. Additionally, the minimal changes in impact strength observed with the “ANT” and “UV” samples compared to the RG8660 samples may be attributed to the relatively low concentration of additives in the samples due to the blending with RG8660 powder. Thus, any potential benefit that either additive may have provided on their own in mitigating mechanical degradation was not clearly detectable.

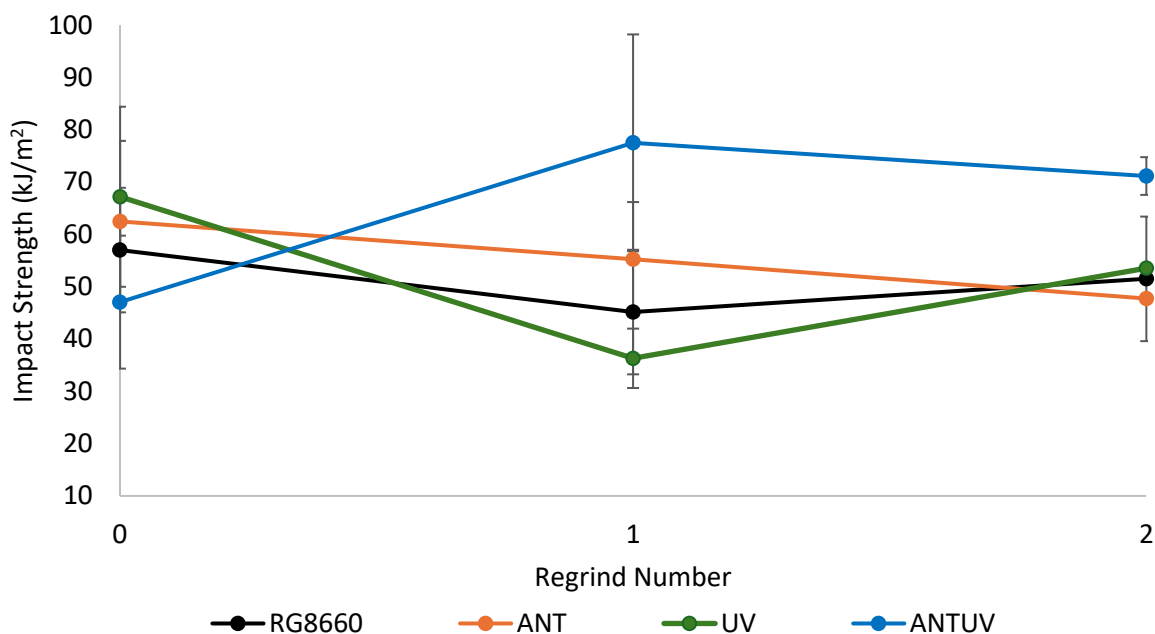


Figure 8.6. Izod impact strength for all of stabilized rotomolded samples compared with RG8660 samples

#### 8.4.4. Yellowness Index Results

The YI was reported for all rotomolded stabilized samples and compared with RG8660 samples, shown in Figure 8.7. There is a notable increase in YI for samples containing antioxidant (ANT and ANTUV) for R0 and R1 samples compared to samples without antioxidant. It has been proven that the intermediate products formed by phenolic antioxidants can significantly increase the YI of samples which may explain this apparent increase in YI observed with the stabilized

samples containing antioxidant. The RG8660 samples displayed a lower overall YI compared to the stabilized samples, further indicating that degradation products alone do not significantly affect the yellowness of the polymer. It is important to recognize that the stabilized samples (ANT, UV and ANTUV) experienced further thermal processing, even before the first rotomolding cycle began, compared to the unstabilized RG8660 sample. Specifically, the stabilized samples had to be processed in a twin-screw extruder for uniform distribution of the additives prior to rotomolding. In contrast, the unstabilized sample was never extruded due to the potential risks involved with uncontrolled crosslinking occurring that would cause damage to equipment. As a result, the baseline comparison of stabilized samples at Regrind 0 involve the polymer exposure to both extrusion and rotomolding, while the unstabilized sample at Regrind 0 involves only rotomolding. Therefore, there is some uncertainty on how much of the yellowing observed for Regrind 0 is attributed to rotomolding but in the absence of a baseline, it will be assumed to be wholly attributed recycling.

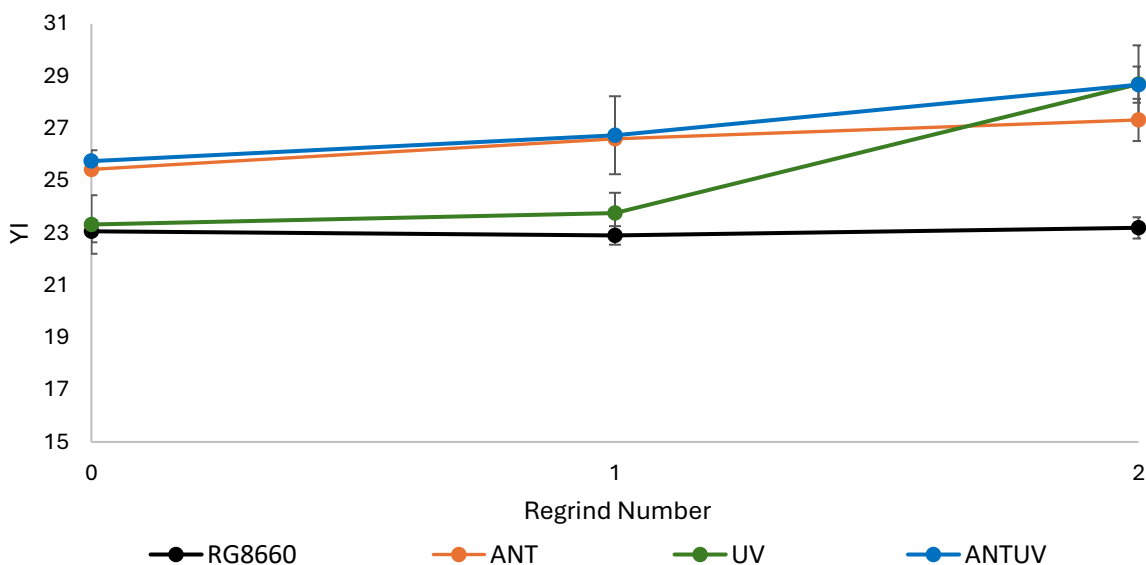


Figure 8.7. YI for all rotomolded stabilized samples compared with RG8660 samples

## 8.5. Conclusions

Overall, the rheological, physical and mechanical properties of the stabilized rotomolded samples were comparable with the unstabilized samples. Minimal improvements in properties may be attributed to the low stabilizer concentrations resulting from blending the extruded material with RG8660. However, this blending was a necessary step prior to rotomolding in order to achieve more uniform particles in the bulk, leading to improved sintering and subsequent uniform wall thicknesses on the final part compared to samples that were rotomolded only using powder obtained from the grinding mill. While no improvements in any properties were detected for samples containing just an antioxidant or UV additive (ANT and UV), the samples containing a combination of both additives (ANTUV) showed minor yet potentially meaningful improvements in sinter-ability as well as an apparent increase in impact strength for the most heavily recycled sample (R2). It is possible that a potential synergy was detected when combining the antioxidants, revealing a significant role of the UV stabilizer in the additive package for alleviating thermo-oxidative degradation effects during rotomolding; however, it is likely that these improvements would be more pronounced with a higher concentration of additives. All samples containing antioxidants (ANT and ANTUV) displayed a noticeable increase in YI compared to samples without antioxidant (RG8660 and UV), confirming the sensitivity that phenolic antioxidants have in yellowing the polymer when exposed to degradation. This further indicates that the YI is an unreliable indicator of the degree of polymer degradation, but instead can be attributed to the by-products formed by the phenolic antioxidants while protecting the polymer from degradation.

## **Chapter 9: Final Conclusions and Future Work**

### **9.1. Final Conclusions**

Two methods of recycling polyethylene regrind were conducted to identify signs of polymer degradation and determine the feasibility of the recycling process. The first method was multi-pass extrusion with a highly stabilized HD 8660.29 resin. Overall, the HD 8660.29 polymer performed with great consistency and observed minimal changes to rheological properties as well as no statistical variation in mechanical properties. It was revealed through the incorporation of a supplementary antioxidant that the virgin HD 8660.29 resin was already heavily stabilized, thus the added antioxidant accumulated on the particles surface, altering the surface chemistry and effectively hindered particle sintering. The stabilizers in the virgin resin were sufficient to avoid depletion during all of the repeated extrusions resulting in minimal deterioration in polymer properties from subsequent rotomolding. While multi-pass extrusion is a classical research technique used by researchers to simulate degradation effects caused by recycling, this method does not fully capture the reality of recycling PIR with rotomolders due to their different processing environments. A better procedure replicating industrial recycling in a rotomolding facility was conducted using the multi-step granulation method with the differently stabilized LL 8555.25 resin. A notable decrease in mechanical properties was only observed for the most heavily recycled material (Regrind 4) while the remaining samples were unaffected. Additionally, the appearance of yellowing was substantial on the final products containing a 50:50 ratio of recycled to virgin resin. This yellowing was found to not be indicative of a degraded polymer, but instead of oxidized by-products of phenolic antioxidant that had been generated during thermal processing.

The role of additives during recycling was further investigated. A completely unstabilized resin was subject to a multi-step granulation recycling process to highlight signs of degradation

and served as a baseline in studies involving the addition of antioxidants. As recycling increased, the unstabilized samples underwent significant alterations in rheological properties, mainly exhibiting increases in viscosities and storage moduli, attributed to crosslinking and branching. Additionally, deterioration in impact strength was observed with increased recycling along with an increasing number of brittle failures during testing. Meanwhile, the heavily degraded recycled samples demonstrated minimal changes in YI, indicating that thermo-oxidative degradation in the absence of stabilizers plays a less significant role in polymer discolouration. The same recycling procedure was then carried out with a blend of a pre-stabilized commercial HDPE resin and an unstabilized HDPE resin to investigate whether the diminishing concentration of stabilizers in the commercial resin with each successive recycling iteration would still be sufficient in mitigating degradation effects. Results revealed that the blends showed notable improvements in rheological and sintering behaviour while the improvements in mechanical properties were not as dramatic.

Finally, a standard antioxidant or UV stabilizer was incorporated into a reactor-grade, unstabilized polyethylene resin to study their individual and combined roles in preventing degradation during recycling. It was determined that the stabilizer concentrations were likely too low to provide dramatic results; however, the UV stabilizer proved to provide synergetic effects in alleviating degradation when combined with the antioxidant which was manifested in an overall improved sintering ability compared to the other samples as well as an apparent improvement in impact strength for the most heavily recycled sample (R2). This synergy may explain the minimal degradation effects observed with recycled HD 8660.29 and LL 8555.25 resins, as discussed in Chapters 4 and 5.

Based on the results obtained from all experiments carried out in this thesis, recycling PIR in rotomolding seems very feasible and can serve as a crucial step in advancing sustainability in



the rotomolding industry. Nonetheless, specific parameters must be considered in order to preserve the quality of the final recycled product. These parameters include the careful selection and concentration of additives corresponding to the degree of recycling anticipated in an industrial facility. UV additives that are commonly combined with antioxidants in commercial resins may inadvertently help alleviate detrimental thermo-oxidative degradation effects during recycling, although additional research involving higher concentrations of additives may be necessary to validate this finding. The concentration of stabilizers is crucial in determining the level of protection from thermo-oxidative degradation during recycling. Concentrations that are too low have proven to not be sufficient in maintaining adequate mechanical performance. However, an excessive concentration of additives may alter the surface tension of the polymer and lead to poor sintering behaviour. While the addition of stabilizers has proven to maintain polymer properties even at high degrees of recycling with a 50:50 virgin to recycled blend ratio, secondary undesirable effects such as polymer discolouration may arise during the course of protecting the polymer from thermo-oxidative degradation due to phenolic antioxidant by-products.

## **9.2.Future Work**

The results revealed in this work provided valuable information about the feasibility of recycling PIR in the rotomolding industry. However, the specific role that different antioxidants play in protecting the polymer from thermo-oxidative degradation effects remains unclear due to the small changes in magnitude of polymer properties revealed through rheological and mechanical analysis. These small variations are likely due to the diminished concentration of additives in a given sample resulting from blending the stabilized material with unstabilized resin for the purpose of achieving greater particle uniformity; studies making direct measures of the additives over each step of recycling would likely be beneficial. Industrial cryogenic grinding of

the stabilized material would be an ideal solution to achieve particle uniformity without the need for blending with unstabilized resin; however, this solution is impractical for a bench-scale study where the material to be ground is minimal. Thus, in order to achieve more definitive conclusions, it is recommended to repeat the additive compounding process with a higher concentration of stabilizers in which a desired target concentration can be reached even after blending with unstabilized polymer.

Furthermore, while the recycling experiments conducted with HD 8660.29 and LL 8555.25 polymer did not display significant signs of mechanical degradation shown by the Izod impact test (presented in Chapters 4 and 5, respectively), the dart impact test is commonly preferred as the industry standard in rotomolding for assessing impact strength since it more closely mimics real-world usage and provides better insight on how well a rotomolded part can withstand drops or collisions. The reason for conducting an Izod impact test over the dart impact test in this thesis was due to the large number of experiments studied in this thesis and the limited resources available for performing the required number of dart impact tests. A future study where less experiments are conducted, such as in the case of only investigating one regrind to virgin blend ratio, the dart impact test would be feasible and could therefore provide better insight on the mechanical performance of recycled rotomolded material in real-world applications.

Finally, the present study is limited to investigating the recyclability of PIR in the rotomolding industry without considering PCR. While the studies with regrind still provided meaningful contributions to advancing sustainability, it is recommended that testing of the recyclability with PCR be considered as the next step since it will have an even greater impact in reducing waste in landfills. Post-consumer plastic waste is a widespread environmental issue across all sectors of the plastic industry; thus, research is required to effectively reintegrate this waste into rotomolding

practices. While there are existing challenges involving PCR in the rotomolding industry, efforts are being made to implement new recycling labels intended for rotomolded PCR which will dramatically boost the recyclability of PCR in the future. It is recommended for future experiments that true rotomolded PCR is sourced and methods are developed to mitigate the extent of degradation manifested through changes in polymer properties, whether it is through the addition of additives into the polymer matrix or blending the recycled material with a pre-stabilized commercial resin.

## References

- Allen, Norman S, Michele Edge, and Sajid Hussain. 2022. "Perspectives on yellowing in the degradation of polymer materials: inter-relationship of structure, mechanisms and modes of stabilisation." *Polymer degradation and stability* 201: 109977.
- Billiani, J, and E Fleischmann. 1990. "Influence of injection rate and melt temperature on polypropylene during injection moulding without packing." *Polymer degradation and stability* 28 (1): 67-75.
- Bolland, JL, and Geoffrey Gee. 1946. "Kinetic studies in the chemistry of rubber and related materials. II. The kinetics of oxidation of unconjugated olefins." *Transactions of the Faraday Society* 42: 236-243.
- Carrero, Julio, Víctor Oliva, Beatriz Navascués, Francesc Borrull, and Marina Galià. 2015. "Determination of antioxidants in polyolefins by pressurized liquid extraction prior to high performance liquid chromatography." *Polymer Testing* 46: 21-25.
- Chen, Changbin, Ruijie Xu, Xiande Chen, Jiayi Xie, Feng Zhang, Yu Yang, and Caihong Lei. 2016. "Influence of cocrystallization behavior on structure and properties of HDPE/LLDPE microporous membrane." *Journal of Polymer Research* 23: 1-9.
- Chen, Lanlan, Xiaojie Sun, Yueqing Ren, Wenbin Liang, and Ke Wang. 2019. "Effects of thermo-oxidative aging on structure and low temperature impact performance of rotationally molded products." *Polymer Degradation and Stability* 161: 150-156.
- Cramez, MC, MJ Oliveira, and RJ Crawford. 2003. "Optimization of the rotational moulding process for polyolefins." *Proceedings of the Institution of Mechanical Engineers, Part B: Journal of Engineering Manufacture* 217 (3): 323-334.
- Crawford, R.J, and J.L. Throne. 2002. *Rotational Molding Technology*. Norwich, New York: William Andrew Publishing.

- Cuadri, AA, and JE Martín-Alfonso. 2017. "The effect of thermal and thermo-oxidative degradation conditions on rheological, chemical and thermal properties of HDPE." *Polymer Degradation and Stability* 141: 1-18.
- Da Costa, Helson M, Valéria D Ramos, and Marisa CG Rocha. 2005. "Rheological properties of polypropylene during multiple extrusion." *Polymer Testing* 24 (1): 86-93.
- Di, Linting, Chenyuan Qin, Wenying Wang, Anping Huang, Fuqing Wei, Huifang Xu, and Shiyuan Yang. 2024. "Influence of Crosslink Density on Electrical Performance and Rheological Properties of Crosslinked Polyethylene." *Polymers* 16 (5): 676.
- Dvorak, Maria. 2016. "Applicability of recycled HDPE for rotational molding."
- Epacher, Edina, János Tolveth, C Kröhnke, and B Pukánszky. 2000. "Processing stability of high density polyethylene: effect of adsorbed and dissolved oxygen." *Polymer* 41 (23): 8401-8408.
- Erbetta, Cynthia D'Avila Carvalho, Getúlio F Manoel, Ana Paula Lelis Rodrigues Oliveira, Maria Elisa Scarpelli Ribeiro e Silva, Roberto Fernando Souza Freitas, and Ricardo Geraldo Sousa. 2014. "Rheological and thermal behavior of high-density polyethylene (HDPE) at different temperatures." *Materials Sciences and Applications* 5 (13): 923.
- Filippone, Giovanni, SC Carroccio, R Mendichi, Lucia Gioiella, N Tz Dintcheva, and Cristian Gambarotti. 2015. "Time-resolved rheology as a tool to monitor the progress of polymer degradation in the melt state—Part I: Thermal and thermo-oxidative degradation of polyamide 11." *Polymer* 72: 134-141.
- Gardette, Mélanie, Anthony Perthue, Jean-Luc Gardette, Tünde Janecska, Enikő Földes, Béla Pukánszky, and Sandrine Therias. 2013. "Photo-and thermal-oxidation of polyethylene:

- Comparison of mechanisms and influence of unsaturation content." *Polymer Degradation and Stability* 98 (11): 2383-2390.
- Gensler, R, CJG Plummer, H-H Kausch, E Kramer, J-R Pauquet, and H Zweifel. 2000. "Thermo-oxidative degradation of isotactic polypropylene at high temperatures: phenolic antioxidants versus HAS." *Polymer Degradation and Stability* 67 (2): 195-208.
- Gijsman, Pieter. 2008. "Review on the thermo-oxidative degradation of polymers during processing and in service." *e-Polymers* 8 (1): 065.
- . 2017. "A review on the mechanism of action and applicability of Hindered Amine Stabilizers." *Polymer Degradation and Stability* 145: 2-10.
- Gugumus, F. 1994. "Mechanisms of thermooxidative stabilisation with HAS." *Polymer degradation and stability* 44 (3): 299-322.
- Horie, K., Máximo Barón, R. B. Fox, J. He, M. Hess, J. Kahovec, T. Kitayama, P. Kubisa, E. Maréchal, W. Mormann, R. F. T. Stepto, D. Tabak, J. Vohlídal, E. S. Wilks, and W. J. Work. 2004. "Definitions of terms relating to reactions of polymers and to functional polymeric materials (IUPAC Recommendations 2003)." *Pure and Applied Chemistry* 76 (4): 889-906. <https://doi.org/doi:10.1351/pac200476040889>.  
<https://doi.org/10.1351/pac200476040889>.
- Inoue, Toshio. 1994. "Selective crosslinking in polymer blends. II. Its effect on impact strength and other mechanical properties of polypropylene/unsaturated elastomer blends." *Journal of applied polymer science* 54 (6): 723-733.
- Kholodovych, Vladyslav, and William J Welsh. 2007. "Thermal-oxidative stability and degradation of polymers." In *Physical properties of polymers handbook*, 927-938. Springer.

- Klemchuk, Peter P, and Paul-Li Horng. 1984. "Perspectives on the stabilization of hydrocarbon polymers against thermo-oxidative degradation." *Polymer degradation and stability* 7 (3): 131-151.
- Kontopoulou, Marianna. 1999. "Polymer Melt Formation and Densification in Rotational Molding." Doctor of Philosophy, McMaster University.
- Mendes, AA, AM Cunha, and CA Bernardo. 2011. "Study of the degradation mechanisms of polyethylene during reprocessing." *Polymer Degradation and Stability* 96 (6): 1125-1133.
- Moss, Serge, and Hans Zweifel. 1989. "Degradation and stabilization of high density polyethylene during multiple extrusions." *Polymer degradation and stability* 25 (2-4): 217-245.
- Odell, JA, A Keller, and AJ Muller. 1992. "Thermomechanical degradation of macromolecules." *Colloid and Polymer Science* 270: 307-324.
- Ogila, KO, M Shao, W Yang, and JJEPL Tan. 2017. "Rotational molding: A review of the models and materials." *Express Polymer Letters* 11 (10).
- Oliveira, MJ, and MC Cramez. 2001. "Rotational molding of polyolefins: Processing, morphology, and properties." *Journal of Macromolecular Science, Part B* 40 (3-4): 457-471.
- Oliveira, MJ, MC Cramez, and RJ Crawford. 1996. "Structure-properties relationships in rotationally moulded polyethylene." *Journal of materials science* 31: 2227-2240.
- Pinheiro, Luís Antonio, Marcelo Aparecido Chinelatto, and Sebastiao Vicente Canevarolo. 2004. "The role of chain scission and chain branching in high density polyethylene during thermo-mechanical degradation." *Polymer Degradation and Stability* 86 (3): 445-453.
- Pospíšil, J, W-D Habicher, J Pilař, S Nešpůrek, J Kuthan, G-O Piringer, and H Zweifel. 2002. "Discoloration of polymers by phenolic antioxidants." *Polymer Degradation and Stability* 77 (3): 531-538.

- Rideal, GR, and JC Padget. 1976. "The thermal-mechanical degradation of high density polyethylene." *Journal of Polymer Science: Polymer Symposia*.
- Sarrabi, Salah, Marie-France Lacrampe, and Patricia Krawczak. 2015. "Phosphorous antioxidants against polypropylene thermal degradation during rotational molding-kinetic modeling." *Journal of Applied Polymer Science* 132 (3).
- Scaffaro, R, FP La Mantia, L Botta, Marco Morreale, N Tz. Dintcheva, and P Mariani. 2009. "Competition between chain scission and branching formation in the processing of high-density polyethylene: Effect of processing parameters and of stabilizers." *Polymer Engineering & Science* 49 (7): 1316-1325.
- Shangguan, Yonggang, Chunhui Zhang, Yanli Xie, Ruifen Chen, Lei Jin, and Qiang Zheng. 2010. "Study on degradation and crosslinking of impact polypropylene copolymer by dynamic rheological measurement." *Polymer* 51 (2): 500-506.
- Sharifi, P, N Henwood, C Liauw, G Lees, and A Quarantino. 2012. "Studies of degradation effects during rotational molding." *Journal of Thermoplastic Composite Materials*.
- Spalding, Mark A, and Ananda Chatterjee. 2017. *Handbook of industrial polyethylene and technology: Definitive guide to manufacturing, properties, processing, applications and markets set*. John Wiley & Sons.
- Turgeon, Dustin. 2024. "rLLDPE for Rotomolding." *The Future of Rotomolding: Making our Industry Innovative and Sustainable*.
- Umbare, Vilas, and Rachayya Arakerimath. 2024. "Investigating the influence of peak internal air temperature (PIAT) on material characteristics of linear low-density polyethylene (LLDPE) during rotational moulding." *Engineering Research Express* 6 (1): 015043.



## Appendix

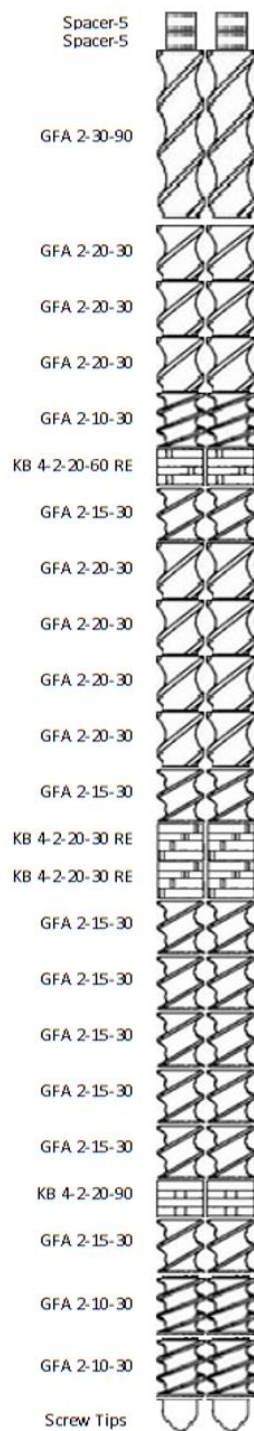


Figure 1A. Screw design used for melt compounding additives with RG8660 polymer, as discussed in Section 8.3.1.